difficulty in WAS patients who have received HST. Furthermore, with 2-color FCM-WASP, MC status could be characterized in different cell lineages. We conclude that FCM-WASP is a useful follow-up method in patients with WAS who have undergone HST. WASP may also have a role in the development of hematopoietic cells in vivo.

Patients, materials, and methods

Patients

The study included 12 patients with a clinical diagnosis of WAS confirmed by genetic studies. The WAS mutations in these patients, some of which were previously reported,[14,16] are listed in Table 1. All patients underwent either cord blood stem cell transplantation (CBT) or bone marrow transplantation (BMT). Transplantation procedures were performed between July 1995 and June 2001 at 6 medical facilities in Japan. The median age of the patients at transplantation was 1.7 years (range, 0.3-4.6 years; Table 1). Five of the 12 patients underwent CBT with cells from an unrelated donor; the rest underwent BMT. The BMT donors were 4 unrelated donors, 2 phenotype-identical mothers (one carrier and one noncarrier), and an identical sister (noncarrier). Four of the 12 patients had a one-antigen–mismatched donor. Preparative regimens and prophylaxis for graft-versus-host disease (GVHD) are shown in Table 1.

Mutation analysis

Genomic DNA was purified from the patients' PBMCs or granulocytes by using Sepa Gene (Sanko Junyaku, Tokyo, Japan). The primers and polymerase chain reaction (PCR) conditions used were described previously.[16] PCR was performed with a GeneAmp PCR system (9700; PE Applied Biosystems, Foster City, CA). Each PCR-amplified fragment was purified from agarose gel and was directly sequenced. Sequencing was performed with an ABI Prism Dye Terminator Cycle Sequencing Ready Reaction kit (PE Applied Biosystems) and an automated ABI 373A DNA analyzer (PE Applied Biosystems).

FCM-WASP

The methods used for FCM-WASP and 2-color FCM-WASP were reported previously.[15] We developed 3-color FCM-WASP for further analysis. Briefly, PBMCs were stained for cell-surface antigens by using the following monoclonal antibodies (mAbs): phycoerythrin (PE)–conjugated anti-CD4, anti-CD8, and anti-CD56 (Southern Biotechnology Associates, Birmingham, AL); PE-conjugated anti-CD20 (Beckman-Coulter, Fullerton, CA); and PE-Cy5–conjugated anti-CD45RA and anti-CD45RO (eBioscience, San Diego, CA). After being washed twice, cells were treated with Cytofix/Cytoperm solution from a CytoStain kit (PharMingen, San Diego, CA) at 4°C for 60 minutes. Cells were then washed twice and incubated with 1:100 diluted anti-WASP (3F3-A5) mAb[17] or purified mouse IgG1 (Becton Dickinson, Mountain View, CA) at 4°C for 30 minutes. The cells were then washed twice and allowed to react with 1:100 diluted fluorescein isothiocyanate–labeled goat anti–mouse IgG1 antibody (Southern Biotechnology Associates) at 4°C for 30 minutes. Stained cells were analyzed with a FACScan flow cytometer using CellQuest software (Becton Dickinson). WASP expression in lymphocytes and monocytes was determined after gating the respective distribution patterns by forward and side scatter (Figure 1A). Because anti-WASP mAb belongs to the mouse IgG1 subclass, all antibodies for staining were of either the mouse IgG2 or IgG3 subclass to avoid a cross-reaction.

Results

Analysis of WAS mutations

Among our 12 patients with WAS, we identified 10 different *WASP* mutations (Table 1). Patient 7 and patient 12 had the same mutation, as did patient 9 and patient 10, although none of these patients' families were related. We reported 5 of these mutations previously[14,16]; 2 mutations (in patients 1 and 4) were novel.

Evaluation of MC status by FCM-WASP

The lymphocyte and monocyte MC status of the WAS patients before and after HST was evaluated by FCM-WASP (Figure 1). Together with $WASP^{bright}$ donor cells, 6 of the 12 patients had $WASP^{dim}$ recipient monocytes and, of these, 5 had $WASP^{dim}$ recipient lymphocytes. In these patients, MC status persisted for at

Table 1. Characteristics of all patients

MC status/ patient no.	Mutation	Year of HST	Age at HST	Nucleated cells transplanted, no.	Donor/ transplant type*	HLA compatibility	Conditioning regimen	GVHD prophylaxis	Acute GVHD grade	Chronic GVHD
With MC status after HST										
1	1 base deletion exon 9†	2001	4 mo	7.5×10^8	U/CBT	5/6 matched	TBI, BuCy, ATG	CsA, Mtx	0	No
2	Missense exon 4 (Ala134-Val)	2000	1 y 2 mo	1.42×10^9	U/CBT	5/6 matched	TBI, Cy, ATG	Mtx, FK506	1	No
3	1 base deletion exon/intron 11; abnormal splice skip exon 11	1999	1 y 2 mo	8.9×10^8	R/BMT	6/6 matched	BuCy, ATG	CsA, Mtx	0	No
4	1 base deletion exon 10†	2001	2 y	2.45×10^8	U/BMT	6/6 matched	TBI, BuCy, ATG	Mtx, FK506	0	No
5	Large deletion	1999	1 y 7 mo	4.8×10^8	U/BMT	5/6 matched	TBI, Cy, ATG	Mtx, FK506	0	Yes
6	Nonsense exon 7 (Arg211-stop)‡	1998	1 y 1 mo	3.34×10^9	U/BMT	6/6 matched	BuCy, ATG	CsA, Mtx	0	No
Without MC status after HST										
7	2 bases deletion exon 1	2000	9 mo	8.8×10^8	U/CBT	5/6 matched	TBI, BuCy, ATG	CsA, PDN	1	No
8	Missense exon 2 (Ile85-Thr)‡	2000	4 y 7 mo	4.2×10^8	U/BMT	6/6 matched	TBI, BuCy, ATG	Mtx, FK506	3	Yes
9	Missense exon 1 (Glu31-Lys)‡	1998	1 y 3 mo	7.0×10^8	U/CBT	6/6 matched	BuCy	CsA, Mtx	1	Yes
10	Missense exon 1 (Glu31-Lys)‡	1996	1 y 7 mo	8.9×10^8	R/BMT	Compatible	BuCy	CsA, Mtx	0	No
11	1 base deletion exon 1‡	1995	4 y 3 mo	8.5×10^9	R/BMT	6/6 matched	BuCy, ATG	CsA, Mtx	0	No
12	2 bases deletion exon 1	2001	7 mo	2.9×10^8	U/CBT	6/6 matched	BuCy, ATG	CsA, PDN	0	No

U indicates unrelated; TBI, total-body irradiation; Bu, busulfan; Cy, cyclophosphamide; ATG, antithymocyte globulin; CsA, cyclosporin A; Mtx, methotrexate; FK506, tacrolimus hydrate; R, related; and PDN, prednisone.

*Related donors were noncarrier mother for patient 3, noncarrier sister for patient 10, and carrier mother for patient 11.

†Novel mutation.

‡Mutation previously reported by us.

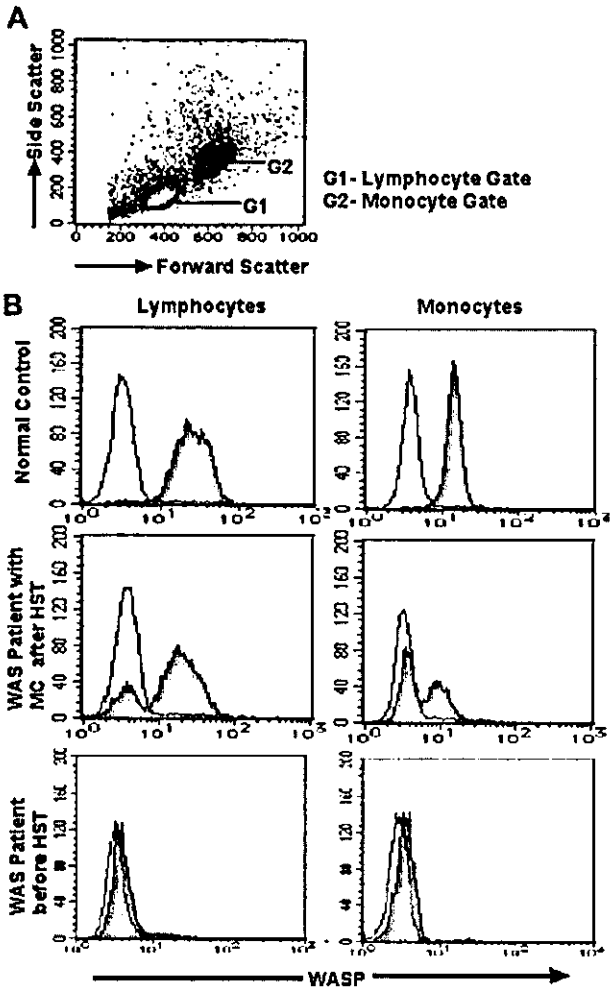

Figure 1. Results of FCM-WASP of lymphocytes and monocytes. (A) Density plot shows forward- and side-scatter data from PBMCs. Lymphocytes (G1 gate) and monocytes (G2 gate) are gated according to the values of these variables. (B) FCM-WASP with a 3-decade log scale. The x-axis represents WASP expression; the y-axis represents cell numbers. The open histogram indicates isotype-control staining; the solid histogram indicates specific staining of WASP. Shown is WASP expression in lymphocytes and monocytes from a healthy control (top), a WAS patient with MC status after HST (middle; data from patient 2 on day 360 after HST), and a WAS patient (patient 12) before HST (bottom).

least 0.5 to 2.5 years after HST. In the other patients, MC status was not observed or observed only transiently. We also performed 2-color FCM-WASP using antibodies to CD4, CD8, CD20, and CD56 (Figure 2). With this method, we were able to characterize in more detail the MC status of these patients according to cell lineage.

Follow-up of patients with MC status in PBMCs

We used 2-color FCM-WASP to follow the 6 patients with MC status for 0.5 to 2.5 years after transplantation (Figure 3). The MC patterns observed varied among the patients, although $WASP^{dim}$ recipient cells were found most frequently in the monocyte population (Table 2). The number of $WASP^{dim}$ recipient lymphocytes and monocytes in patient 1 appeared to diminish gradually, indicating that all hematopoietic cells would eventually be replaced by donor cells. In patients 2 and 5, we observed stable MC status with regard to monocytes, of which approximately half were found to be recipient cells. In contrast, most of the lymphocytes were $WASP^{bright}$ donor cells. Patient 2 had a transient increase in $CD4^+$ $WASP^{dim}$ recipient cells at day 360 after HST, which was correlated with a $WASP^{bright}$ donor $CD4^+$ increment (data not shown). The same phenomenon was observed on a different day after HST in patient 1. In patients 3 and 4, the monocytes were mostly $WASP^{dim}$, whereas most of their lymphocytes were $WASP^{bright}$, except for the $CD20^+$ cells in patient 3. The precise MC status in patient 3, who consistently had $WASP^{dim}$ lymphocytes, is shown in Figure 4. It was noteworthy that most of his $CD20^+$ cells were $WASP^{dim}$. In patient 4, we observed a surprising conversion of the dominant proportion of monocytes from $WASP^{bright}$ to $WASP^{dim}$ 30 to 190 days after HST. Patient 6, who underwent HST more than 900 days before testing, had no recipient cells of any lymphocyte lineage, whereas approximately 10% of his monocytes remained $WASP^{dim}$.

Evaluation of MC status of granulocytes and platelets

Because of unknown technical reasons, FCM-WASP could not be used to detect WASP in myeloid cells. Instead, we tried to evaluate the MC status of the patients' granulocytes by directly sequencing DNA from these cells. This method could be used for every patient except patient 5, whose mutation was a large deletion of the *WASP* gene. However, donor type (sex and carrier status) must be taken into account for this evaluation; a cell from a male donor has a wild-type WASP allele, a normal cell from a female donor has 2 wild-type WASP alleles, and a cell from a female carrier has a mutant and a wild-type WASP allele. The MC status of the patients'

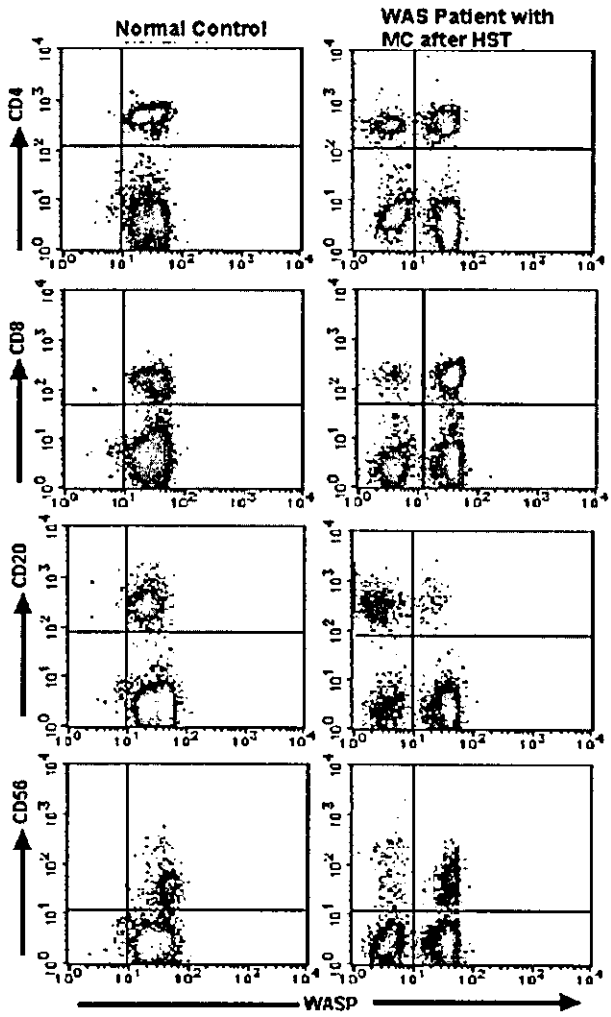

Figure 2. Results of 2-color FCM-WASP. Density plots are from 2-color FCM-WASP using CD4, CD8, CD20, and CD56 antibodies. All cells in the lymphocyte gate were analyzed. The x-axis represents WASP intensity; the y-axis represents the intensity of the respective CD marker. Shown are the results for patient 3 on day 720 after HST.

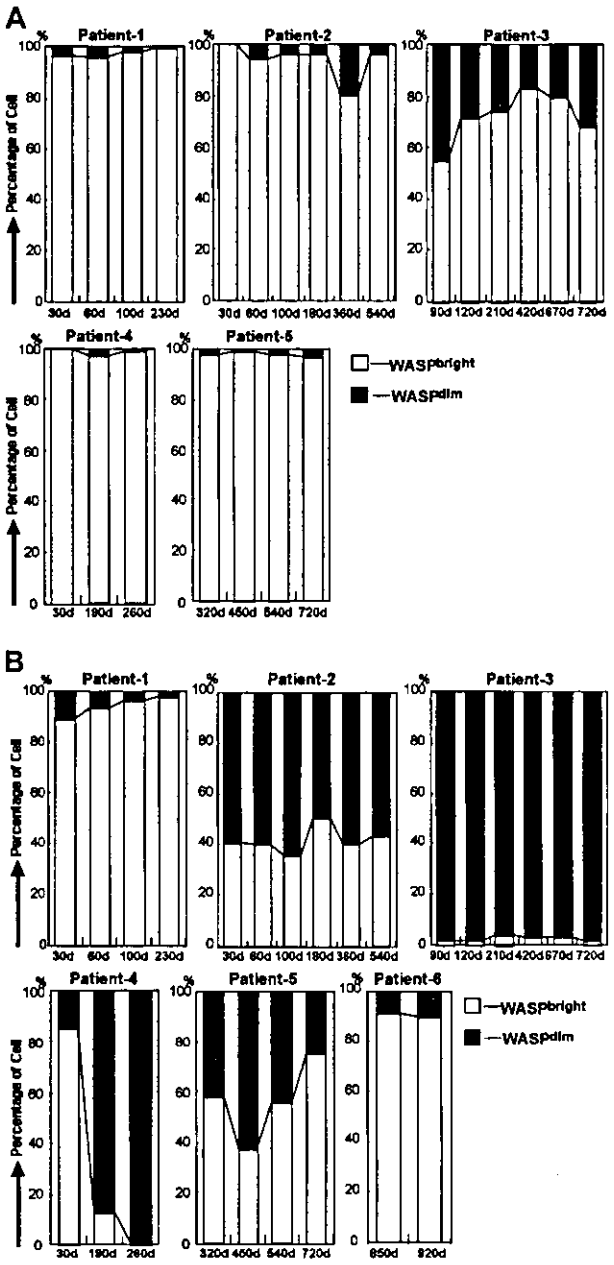

Figure 3. Follow-up studies in patients with MC status after HST. (A) Bar charts show changes in MC status in lymphocytes obtained from 5 WAS patients after HST. Open bars and solid bars depict the proportion of lymphocytes with $WASP^{bright}$ donors and $WASP^{dim}$ recipients, respectively. (B) Bar charts show changes in MC status in monocytes obtained from 6 WAS patients after HST. Open bars and solid bars depict the proportion of monocytes with $WASP^{bright}$ donors and $WASP^{dim}$ recipients, respectively.

granulocytes as evaluated by this method correlated roughly with that of his monocytes on FCM-WASP (Table 2). After HST, most patients showed an increase in the number of platelets with a normal mean volume. However, patients 3 and 4, most of whose monocytes and granulocytes were $WASP^{dim}$, had persistent thrombocytopenia (Table 2).

MC status in bone marrow

Results of evaluations of MC status in bone marrow by fluorescence in situ hybridization (FISH) or polymorphic analysis with short tandem repeats are summarized in Table 2. Use of this method revealed that in patients 3 and 4, 84% to 90% of the bone marrow cells were of recipient origin. These patients are now being scheduled to receive a second HST.

Immunologic evaluation of patients who underwent HST

Serum IgM and IgE levels in patients before and after HST are shown in Table 3. After HST, most patients, including those with MC status, had an increase in serum IgM levels and a decrease in serum IgE levels. In patients 3, 4, and 8, however, serum IgE levels did not normalize after HST.

Naive/memory T cells of patients after HST

To determine the naive/memory profile of the donor and recipient T cells in the patients after HST, we performed 3-color FCM-WASP with anti-CD45RA or anti-CD45RO antibodies for each population of $CD4^+$ and $CD8^+$ T cells. We found that $WASP^{bright}$ donor T cells developed into $CD45RA^-/CD45RO^+$ memory cells during the first year after HST (Figure 5). In contrast, most of the $WASP^{dim}$ recipient T cells (both $CD4^+$ and $CD8^+$) remained $CD45RA^+/CD45RO^-$ (naive) cells, even after more than a year. The results in patients 1, 2, and 3 at 230, 540, and 720 days, respectively, after HST are shown in Figure 5. These findings were more striking in $CD4^+$ cells than in $CD8^+$ cells.

Discussion

We here report an evaluation of MC status in 12 patients with WAS who underwent HST. With FCM-WASP, donor and recipient PBMCs could be distinguished easily. Moreover, the MC status of these patients according to cell lineage was characterized by using 2-color FCM-WASP. Although several follow-up studies in WAS patients who have undergone HST have been reported,[12,18,19] this is the first study in which MC status of these patients was evaluated precisely. We found that 6 of the 12 patients with WAS evaluated (50%) had MC status lasting for at least 7 months (maximum, 2.5 years).

Ozsahin et al[18] studied the outcome of BMT in patients with WAS and reported that 7 of 23 patients (30.4%) showed MC status, although these patients were not characterized in detail. Several factors likely contribute to the rate of MC status after BMT. The higher rate of MC status in our study, however, may be due to use of the FCM-WASP procedure, which seems to be more sensitive in detecting recipient cells than the method used in previous studies.

Findings in the WAS patients we studied who were positive for MC status are summarized in Table 2. The residual recipient cells were detected most consistently in the monocyte population. These results are consistent with those of our previous studies, which concluded that WAS carriers have a mixed population of $WASP^{dim}$ and $WASP^{bright}$ monocytes, whereas most carriers have no detectable $WASP^{dim}$ cells in the lymphocyte compartment.[13,14] We speculate that there are in vivo differences among the hematologic cell lineages in their dependence on WASP during development and that monocytes are somehow less dependent on WASP than are other PBMCs. It is noteworthy that the dominant population among $CD20^+$ cells in patient 3 was $WASP^{dim}$. This may help pinpoint the position of B cells in the hierarchy of WASP dependency among the hematopoietic cells (monocytes have less WASP dependency than B cells, which have less WASP dependency than other lymphocytes).

We retrospectively surveyed our patients in an attempt to find other factors that could be related to MC status after HST. No significant differences were detected in type of mutation, type of donor, number of cells transplanted, regimen used for conditioning,

Table 2. Findings in patients with MC status

Patient no.	Recipient cells, %*		Results of sequencing DNA from granulocytes	Recipient cells in BM, %	Platelet no., × 10^9/L/platelet vol, fL	
	Lymphocytes	Monocytes			Before HST	After HST
1	1 (230)	2 (230)	Normal ≫ mutation (30)	ND	2.1/5.3	35.9/8.8 (104)
2	4 (540)	60 (540)	Mutation = normal (230)	68 (260)	1.4/5.4	10.8/7.3 (671)
3	20 (720)	99 (720)	Mutation ≫ normal (720)	90 (730)	1.1/5.2	2.8/ND (720)
4	0.6 (260)	99 (260)	Mutation ≫ normal (260)	85 (170)	4.0/5.2	2.2/4.4 (279)
5	3.5 (720)	25 (720)	NA	32 (310)	3.1/6.4	11.0/(ND) (655)
6	0 (920)	10 (920)	ND	ND	4.3/5.9	25.0/8.5 (859)

Values in parentheses are the number of days after HST.
BM indicates bone marrow; ND, not determined; and NA, not available because of a large deletion mutation.
*$WASP^{dim}$ on FCM-WASP.

or grade of GVHD (Table 1). We found a difference in the proportion of cells of the $WASP^{bright}$ donor cell lineage in the early phase after HST. Most patients without MC status or with transient MC status had a high number of $CD56^+$ cells among their $WASP^{bright}$ donor cell populations (more than 50% earlier than day 90 after HST; data not shown). In contrast, in all patients with MC status except patient 1, $CD56^+$ cells comprised less than 10% of the $WASP^{bright}$ donor population at that time (data not shown). It was previously reported that $CD56^+$ cells recovered earlier than cells of other lineages (such as $CD8^+$, $CD4^+$, and $CD20^+$ cells) after unrelated CBT.[20] We do not know the mechanism involved, but these cells may help to provide favorable conditions for engraftment of donor cells after HST. On the other hand, the initial development of $CD56^+$ cells may be an indicator of earlier engraftment and growth of donor hematologic stem cells of that lineage than of other lineages. It is possible that these cells are actually mature donor T cells that are mixed in during transplantation.[21]

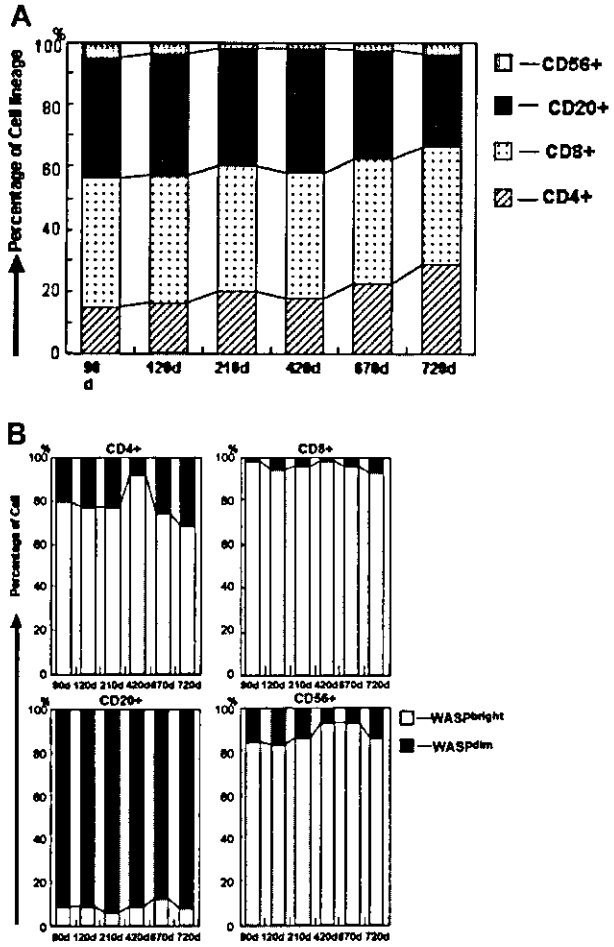

Figure 4. Evaluation of the precise MC status in patient 3. (A) Change in lymphocyte subsets (combined $WASP^{bright}$ and $WASP^{dim}$ cells) in patient 3 after HST. The 4 patterns in the bar show the proportions of $CD4^+$, $CD8^+$, $CD20^+$, and $CD56^+$ cells, respectively. (B) Change in MC status in each lymphocyte subset of $CD4^+$, $CD8^+$, $CD20^+$, and $CD56^+$ cells. Shown is the proportion of $WASP^{bright}$ donors (open bars) and $WASP^{dim}$ recipients (solid bars) in each subset.

We were not able to measure WASP expression in granulocytes by FCM-WASP for unknown reasons. There is controversy regarding whether mature granulocytes express WASP in their cytoplasm.[5] However, the recent finding of X-linked neutropenia with WASP mutation (L270P) may indicate that WASP is at least expressed in myeloid precursor cells.[22] To evaluate the MC status of granulocytes, we sequenced DNA from purified granulocytes from some of our patients with WAS. By comparing nucleotide signals of the wild-type and mutant at the mutation site and taking donor type into consideration, we could estimate roughly the proportion of donor and recipient cells in this cell population.[15] The granulocyte proportion of donor to recipient cells seemed similar to that of the monocyte proportion (Table 2). We also evaluated platelet status after HST by assessing platelet numbers and mean volume. Although WASP expression in platelets was not studied, the origin of platelets after HST looked the same as that of monocytes. The number of platelets correlated roughly with the proportion of $WASP^{bright}$ in monocytes. After HST, persistent thrombocytopenia was observed in patients 3 and 4, and patients 2 and 5 had slightly low platelet counts (Table 2). We think that these results together indicate that the precursors of both granulocytes and platelets, similar to those of monocytes, are less WASP dependent during their development than are lymphocyte precursors.

Table 3. Immunologic results in patients with WAS before and after HST

Patient no.	IgM (g/L)		IgE (kU/L)	
	Before HST	After HST	Before HST	After HST
1	0.48	1.44 (377)	2200	58 (391)
2	0.18	2.46 (666)	100	< 5 (505)
3	0.37	1.58 (832)	1100	930 (882)
4	0.24	1.45 (188)	1800	500 (286)
5	0.79	0.65 (652)	230	69 (634)
6	0.63	1.53 (859)	6652	45 (859)
7	< 0.18	1.14 (579)	115	47 (148)
8	0.24	0.80 (476)	36	1100 (559)
9	0.22	0.93 (1187)	732	< 2 (1187)
10	0.46	0.89 (1963)	3372	47 (1963)
11	0.31	0.58 (2229)	600	56 (2229)
12	0.22	0.70 (117)	732	6 (117)

Values in parentheses are the number of days after HST.

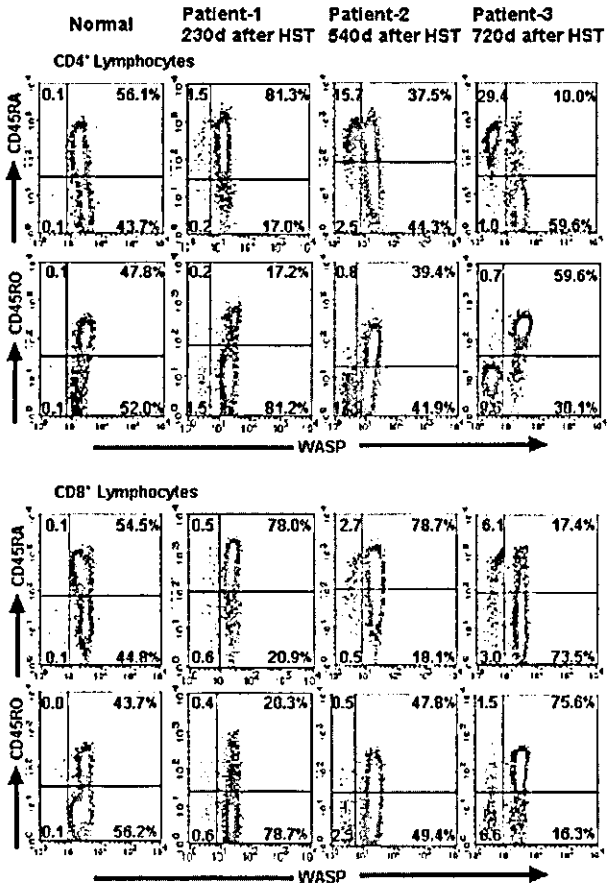

Figure 5. Evaluation of the naive and memory profile of T cells in WAS patients after HST. Density plots from 2-color immunofluorescence depict the results of 3-color FCM-WASP using anti-CD45RA or anti-CD45RO for each population of $CD4^+$ and $CD8^+$ T cells. All cells pictured were gated with a forward- and side-scatter lymphocyte gate combined with a $CD4^+$ or $CD8^+$ gate. The x-axis represents WASP staining intensity; the y-axis represents CD45RA or CD45RO expression. Numbers within the density plots represent the percentage of cells in each quadrant. It is noteworthy that in contrast to the $WASP^{bright}$ donor $CD4^+$ and $CD8^+$ cells, most $WASP^{dim}$ recipient cells in patients 1, 2, and 3 remained $CD45RA^+/CD45RO^-$ (naive) at the indicated days after HST.

The MC status of the bone marrow of some patients (2, 3, 4, and 5) was studied by using FISH or short tandem repeat analysis (Table 2). It is noteworthy that the proportion of recipient cells in bone marrow was approximately equal to that of monocytes studied by using FCM-WASP. Therefore, the peripheral blood monocyte profile may accurately represent MC status of the bone marrow in WAS patients after HST. As previously reported,[14] patient 11 received hematopoietic stem cells from his carrier mother, and 10% to 20% of his monocytes were subsequently found to be $WASP^{dim}$. However, karyotype analysis showed that these cells were actually derived from donor hematopoietic stem cells. The same $WASP^{dim}$ proportion was observed in monocytes from the patient's mother. Thus, in cases in which the donor is a WAS carrier, this problem must be taken into account when determining MC status. In patients 3 and 4, most of the donor cells appeared to be rejected, yet the lymphocytes in these patients were found to be predominantly $WASP^{bright}$ cells of donor origin (except the $CD20^+$ cells in patient 3), suggesting again that WAS protein provides lymphocytes with a strong growth or survival advantage during development or circulation.

Using 3-color FCM-WASP, we evaluated the naive ($CD45RA^+/RO^-$) and memory/activated ($CD45RA^-/RO^+$) subsets of the patients' recipient and donor peripheral $CD4^+$ and $CD8^+$ cells. Patients who underwent HST had naive donor T cells in their peripheral blood after 6 months. These cells were found to develop into memory/activated T cells during the next 6 months. In contrast, most recipient T cells remained $CD45RA^+/RO^-$ (naive) a full year after HST; these findings were more striking in $CD4^+$ cells than in $CD8^+$cells. Patients with WAS were previously found to have a marked number of $CD45RA^-/RO^+$ T cells in their peripheral blood before HST.[22] We also observed this in 2 of the patients we examined before HST, whose ratio of $CD45RA^+/RO^-$ to $CD45RA^-/RO^+$ cells was comparable to that in age-matched controls (data not shown). Thus, the results obtained with 3-color FCM-WASP in this study may represent the outcome under a condition of competition between $WASP^{bright}$ and $WASP^{dim}$ memory T cells. The same phenomenon was observed during a study of somatic mosaicism induced by genetic reversion in a patient with WAS.[23] Although the patient's $CD45RA^+$ T cells consisted of an even number of $WASP^{bright}$ and $WASP^{dim}$ cells, most of the $CD45RO^+$ T cells (> 90%) were $WASP^{bright}$. Together, these results suggest that $WASP^{bright}$ T cells have a growth advantage over $WASP^{dim}$ T cells after stimulation with antigens, although a shortened lifespan of $WASP^{dim}$ memory T cells as a result of spontaneous apoptosis could also be responsible.[24,25]

Finally, we examined serum IgM and IgE levels in our patients before and after HST to evaluate immunologic status. Most patients, including those with MC status, had an increase in serum IgM and a decrease in serum IgE levels after HST. It is interesting that patient 3 also had a marked increase in IgM. Because most of his B cells and monocytes, but not his T cells, were $WASP^{dim}$, this finding may indicate that $WASP^{bright}$ T cells, especially memory T cells, play a key role in normal IgM production in WAS patients after HST. Contrary to our expectations, however, patients 3 and 4 regained approximately the same IgE levels, and patient 8 had an increase in IgE after HST. A larger number of cases are required to assess the use of IgE levels for immunologic evaluations after HST, because regulation of IgE seems to be complicated and WASP is not the only molecule involved in this process.

We conclude that FCM-WASP is a useful method for follow-up of patients with WAS who have undergone HST. Our findings may also have important implications regarding the in vivo role of WASP during the development of hematopoietic cells.

Acknowledgments

We thank Professor K. Kobayashi for critical comments on this article and the medical staff for excellent patient care.

References

1. Wiskott A. Familiärer, angeborener morbus Werlhofii. Monatsschr Kinderheilkd. 1937;68:212-216.
2. Aldrich RA, Steinberg AG, Campbell DC. Pedigree demonstrating a sex-linked recessive condition characterized by draining ears, eczematoid dermatitis and bloody diarrhea. Pediatrics. 1954; 13:133-139.
3. Sullivan KE, Mullen CA, Blaese RM, Winkelstein JA. A multiinstitutional survey of the Wiskott-Aldrich syndrome. J Pediatr. 1994;125:876-885.
4. Derry JM, Ochs HD, Francke U. Isolation of a novel gene mutated in Wiskott-Aldrich syndrome. Cell. 1994;78:635-644.
5. Shcherbina A, Rosen FS, Remold-O'Donnell E. WASP levels in platelets and lymphocytes of Wiskott-Aldrich syndrome patients correlate with cell dysfunction. J Immunol. 1999;163:6314-6320.

6. Cory GO, MacCarthy-Morrogh L, Banin S, et al. Evidence that the Wiskott-Aldrich syndrome protein may be involved in lymphoid cell signaling pathways. J Immunol. 1996;157:3791-3795.
7. Symons M, Derry JM, Karlak B, et al. Wiskott-Aldrich syndrome protein, a novel effector for the GTPase CDC42Hs, is implicated in actin polymerization. Cell. 1996;84:723-734.
8. Molina IJ, Sancho J, Terhorst C, Rosen FS, Remold-O'Donnell E. T cells of patients with the Wiskott-Aldrich syndrome have a restricted defect in proliferative responses. J Immunol. 1993; 151:4383-4390.
9. Simon HU, Mills GB, Hashimoto S, Siminovitch KA. Evidence for defective transmembrane signaling in B cells from patients with Wiskott-Aldrich syndrome. J Clin Invest. 1992;90:1396-1405.
10. Gallego MD, Santamaria M, Pena J, Molina IJ. Defective actin reorganization and polymerization of Wiskott-Aldrich T cells in response to CD3-mediated stimulation. Blood. 1997;90:3089-3097.
11. Kenney D, Cairns L, Remold-O'Donnell E, Peterson J, Rosen FS, Parkman R. Morphological abnormalities in the lymphocytes of patients with the Wiskott-Aldrich syndrome. Blood. 1986;68:1329-1332.
12. Filipovich AH, Stone JV, Tomany SC, et al. Impact of donor type on outcome of bone marrow transplantation for Wiskott-Aldrich syndrome: collaborative study of the International Bone Marrow Transplant Registry and the National Marrow Donor Program. Blood. 2001;97:1598-1603.
13. Yamada M, Ohtsu M, Kobayashi I, et al. Flow cytometric analysis of Wiskott-Aldrich syndrome (WAS) protein in lymphocytes from WAS patients and their familial carriers [letter]. Blood. 1999;93: 756-757.
14. Yamada M, Ariga T, Kawamura N, et al. Determination of carrier status for the Wiskott-Aldrich syndrome by flow cytometric analysis of Wiskott-Aldrich syndrome protein expression in peripheral blood mononuclear cells. J Immunol. 2000;165: 1119-1122.
15. Ariga T, Kondoh T, Yamaguchi K, et al. Spontaneous in vivo reversion of an inherited mutation in the Wiskott-Aldrich syndrome. J Immunol. 2001; 166:5245-5249.
16. Ariga T, Yamada M, Sakiyama Y. Mutation analysis of five Japanese families with Wiskott-Aldrich syndrome and determination of the family members' carrier status using three different methods. Pediatr Res. 1997;41:535-540.
17. Stewart DM, Treiber-Held S, Kurman CC, Facchetti F, Notarangelo LD, Nelson DL. Studies of the expression of the Wiskott-Aldrich syndrome protein. J Clin Invest. 1996;97:2627-2634.
18. Ozsahin H, Le Deist F, Benkerrou M, et al. Bone marrow transplantation in 26 patients with Wiskott-Aldrich syndrome from a single center. J Pediatr. 1996;129:238-244.
19. Mullen CA, Anderson KD, Blaese RM. Splenectomy and/or bone marrow transplantation in the management of the Wiskott-Aldrich syndrome: long-term follow-up of 62 cases. Blood. 1993;82: 2961-2966.
20. Thomson BG, Robertson KA, Gowan D, et al. Analysis of engraftment, graft-versus-host disease, and immune recovery following unrelated donor cord blood transplantation. Blood. 2000;96: 2703-2711.
21. Rufer N, Helg C, Chapuis B, Roosnek E. Human memory T cells: lessons from stem cell transplantation. Trends Immunol. 2001;22:136-141.
22. Gerwin N, Friedrich C, Perez-Atayde A, Rosen FS, Gutierrez-Ramos JC. Multiple antigens are altered on T and B lymphocytes from peripheral blood and spleen of patients with Wiskott-Aldrich syndrome. Clin Exp Immunol. 1996;106:208-217.
23. Wada T, Schurman SH, Otsu M, et al. Somatic mosaicism in Wiskott-Aldrich syndrome suggests in vivo reversion by a DNA slippage mechanism. Proc Natl Acad Sci U S A. 2001;98:8697-8702.
24. Rawlings SL, Crooks GM, Bockstoce D, Barsky LW, Parkman R, Weinberg KI. Spontaneous apoptosis in lymphocytes from patients with Wiskott-Aldrich syndrome: correlation of accelerated cell death and attenuated bcl-2 expression. Blood. 1999;94:3872-3882.
25. Rengan R, Ochs HD, Sweet LI, et al. Actin cytoskeletal function is spared, but apoptosis is increased, in WAS patient hematopoietic cells. Blood. 2000;95:1283-1292.

British Journal of Haematology, 2002, 118, 858–863

The role of common gamma chain in human monocytes *in vivo*; evaluation from the studies of X-linked severe combined immunodeficiency (X-SCID) carriers and X-SCID patients who underwent cord blood stem cell transplantation

TADASHI ARIGA,[1] KOJI YAMAGUCHI,[1] JUKEI YOSHIDA,[1] AKIHIKO MIYANOSHITA,[2] TOSHIHIDE WATANABE,[3] TADASHI DATE,[4] JUNE-ICHI MIURA,[5] SATORU KUMAKI,[6] NAOTO ISHII[7] AND YUKIO SAKIYAMA[1,2] [1]*Research Group of Human Gene Therapy, Hokkaido University Graduate School of Medicine,* [2]*Department of Paediatrics, Teine Keijinkai Hospital, Sapporo,* [3]*Department of Paediatrics, Hokkaido Children's Hospital and Medical Centre, Otaru,* [4]*Department of Paediatrics, Kurume Medical College, Kurume,* [5]*Department of Paediatrics, Asahikawa Red Cross Hospital, Asahikawa,* [6]*Department of Paediatric Oncology, Institute of Development, Ageing and Cancer, Tohoku University, and* [7]*Department of Immunology, Tohoku University School of Medicine, Sendai, Japan*

Received 28 November 2001; accepted for publication 13 March 2002

Summary. Expression of common gamma chain (γc) on monocytes was studied in five carriers of X-linked severe combined immunodeficiency (X-SCID) and two X-SCID patients who underwent cord blood stem cell transplantation (CBSCT). Flow cytometric analysis revealed that both γc-negative and positive monocytes co-existed in X-SCID carriers, whereas no γc-negative T, B or NK cells were observed in them. Clonal analysis and reverse transcription polymerase chain reaction studies revealed that 13·2–45·0% of monocytes from these carriers expressed the mutant γc message. X-SCID patients who received CBSCT persistently possessed the majority of γc-negative monocytes with a good clinical course. These results, together, may indicate that γc is not essential for monocyte development/function *in vivo*.

Keywords: X-SCID, carrier, monocyte, common gamma chain, haematopoietic stem cell transplantation.

Common gamma chain (γc), its cording gene located in Xq13, is an essential component of the receptors for interleukins 2, 4, 7, 9, 15 and 21 (Leonard *et al*, 1995; Sugamura *et al*, 1995; Malek *et al*, 1999; Asao *et al*, 2001). Inherited defect of this molecule causes X-linked severe combined immunodeficiency (X-SCID) (Noguchi *et al*, 1993; Puck *et al*, 1993), which is characterized by the absence of mature T and natural killer (NK) cells with a normal/increased number of dysfunctional B cells in peripheral blood. X-SCID patients can successfully be treated by haematopoietic stem cell transplantation (HSCT). Even after successful HSCT, however, it has been revealed that most X-SCID patients persistently possessed γc-negative B cells (Haddad *et al*, 1999), indicating that this molecule is essential for T and NK cells, but not for B cells *in vivo*. In contrast to human γc, mouse γc is essential for B-cell development. It was clearly demonstrated by experimental models (Otsu *et al*, 2000) and, in fact, mature B cells are totally absent in the X-SCID mouse (Cao *et al*, 1995; DiSanto *et al*, 1995). These observations are good illustrations to show that destruction of the equivalent molecule between mouse and human results in different phenotypes. The important role of γc in human B-cell development *in vivo*, however, is highlighted in X-SCID carriers. It has been revealed that B cells, as well as T and NK cells, of X-SCID carriers showed the severe skewed X inactivation pattern, which suggested that no γc-negative B, T or NK cells developed in carriers (Conley *et al*, 1988; Wengler *et al*, 1993). These findings indicated that human B cells with a defective γc molecule ultimately show growth disadvantage against those with normal γc molecule in the impartial condition *in vivo*.

In contrast to the well-characterized role of γc in T, B and NK cells, that of γc in monocytes has not been fully understood (Bonder *et al*, 1998; Bonder *et al*, 1999). The

Correspondence: Dr Tadashi Ariga, Research Group of Human Gene Therapy, Hokkaido University School of Medicine, N-15, W-7, Kita-ku Sapporo, 060–8638, Japan. E-mail: tada-ari@med.hokudai.ac.jp

number of monocytes in X-SCID patients is not reduced, similar to their B cells. However, no precise studies for the monocyte profile in X-SCID carriers have been reported. It has not been clarified whether X-SCID patients would replace γc-negative monocytes with γc-positive monocytes after successful HSCT (Buckley *et al*, 1999; Haddad *et al*. 1999).

To investigate the role of γc in human monocytes, we studied five X-SCID carriers from four different families and two X-SCID patients, who had received cord blood stem cell transplantation (CBSCT) to determine whether they possessed monocytes expressing the mutant γc gene. Flow cytometric and reverse transcription polymerase chain reaction (RT-PCR) studies revealed that a significant portion of monocytes from these carriers consisted of γc-negative cells, and the patients after CBSCT, persistently possessed a majority of γc-negative monocytes. These results, together, may indicate that γc is dispensable for human monocyte development/function *in vivo*.

MATERIALS AND METHODS

X-SCID carriers. Five carriers from four different families (A, B, C and D) were studied. They were a mother and a sister of an X-SCID patient from family A (carriers A1 and A2), and three mothers of X-SCID patients from families B, C and D (carriers B, C and D). All the patients were clinically diagnosed as X-SCID, and confirmed by molecular genetic studies. The mutations of γc gene detected in X-SCID patients (from families A, B, C and D) were E68K (GAG → AAG), S108P (TCT → CCT), 771(+1)G → T of intron 5 and deletion of 391A respectively (Kumaki *et al*, 2000). Carrier diagnosis was performed based on genetic studies after informed consent. All the four mutations resulted in a lack of γc on the cell surface. The mutation of 771(+1)G → T of intron 5 resulted in a skipping out of exons 4 and 5 from the γc message (Kumaki *et al*. 2000).

X-SCID patients. X-SCID patients A and C, who had received CBSCT without any conditioning, were included in the study. After the transplantation, both patients made satisfactory progress without serious side-effects or severe infectious episodes. At 1 and 3 years after the transplantation, respectively, γc expression on their monocytes was studied. The patients from families B and D were not available because they died of severe infectious diseases soon after the diagnosis.

Flow cytometric analysis for γc expression. Peripheral blood mononuclear cells (PBMC), washed with 1% fetal bovine serum/phosphate-buffered saline (FBS/PBS), were incubated with 2% of human IgG (Venilon®) for blocking, and stained with a biotin-conjugated rat anti-γc monoclonal antibody (mAb) (TUGh4, Pharmingen, San Diego, CA, USA) (Ishii *et al*, 1994) at 4°C for 30 min. After washing twice with cold 1% FCS/PBS, the cell pellets were re-suspended in PBS containing diluted streptavidin-phycoerythrin (Becton Dickinson Immunocytometry Systems, San Jose, CA, USA) at 4°C for 30 min. Biotin rat IgG2a (CEDARLANE®, Hornby, Canada) was used as an isotypic control Ab. For dual staining of the T, B and NK cells, the above cells were further washed and incubated with diluted fluorescein isothiocyanate (FITC)-conjugated mouse anti-CD4, CD8, CD20 (Becton Dickinson Immunocytometry Systems) and CD56 (Southern Biotechnology Associates, Inc. Birmingham, AL, USA) mAb respectively. A forward scatter/side scatter (FSC/SCC) profile was used for gating monocytes.

Cell separation. PBMC were separated by centrifugation on Ficoll-Hypaque gradient. T, B cells and monocytes used for RNA purification were purified from PBMC using anti-CD3, -CD20 and -CD14 magnetic beads (Miltenyi Biotec, Auburn, CA, USA) respectively. Purity of these cells was confirmed by flow cytometry.

Detection of the mutant γc message in monocytes from four X-SCID carriers. Total RNA was purified from $CD3^+$, $CD20^+$ and $CD14^+$ cells using TRIZOL® (Life Technologies, Inc. Grand Island, NY, USA), and then cDNA from each 1 μg of RNA was synthesized (First-strand cDNA synthesis kit; Amersham Pharmacia Biotech, Buckinghamshire, UK). The γc cDNA, including the mutation sites of carriers A1, A2 and B, was amplified by RT-PCR with primers γc cDNA121F; CCACAGCTGATTTCTTCCTG and γc cDNA454R; TTTAGCATCTGTGTGGCCTG. It was confirmed that genomic fragments were not amplified with the primers above. The amplified products were then cloned into the TA vector (PCR2·1; Invitrogen, Carlsbad, CA, USA). Seven to 41 clones derived from $CD3^+$, $CD14^+$ and $CD20^+$ cells from the carriers were sequenced. For carrier C, RT-PCR with primers γc cDNA121F; CCACAGCTGATTTCTTCCTG and γc cDNA 820R; GAGCCAACAGAGATAACCAC was performed. Because exons 4 and 5 were spliced out from the mutant γc message (Kumaki *et al*, 2000), it was easily distinguished on the gel from the normal one after electrophoresis (700 bp *vs* 397 bp).

Sequencing studies. Purified RT-PCR products or clones including the γc cDNA were sequenced with primer γc cDNA121F, using an Applied Biosystem Prism Dye Terminator Cycle Sequencing kit (Applied Biosystem, Foster City, CA, USA) and an ABI PRISM 310 Genetic Analyser (Applied Biosystem).

RESULTS

Flow cytometric analysis of X-SCID carriers

γc was positive on monocytes from healthy controls; it was detected as the normal distribution pattern (dull peak; Fig 1), whereas it was absent on those from X-SCID patient A before HST (sharp peak; Fig 1). Monocytes from carriers showed the mixed pattern of controls and patients (the medium fluorescent intensity values and geometric means are indicated in Table I), suggesting the presence of two monocyte populations with a positive and negative γc molecule (Fig 1). When gated for lymphocytes by FSC/SSC profiles, there were no differences for γc expression between the controls and carriers; both groups showed the only positive population (data not shown). Further analysis of dual staining of γc with several CD markers indicated that no γc-negative population was detected in $CD4^+$, $CD8^+$, $CD20^+$ or $CD56^+$ cells in all the carriers (data for carrier A1 is shown in Fig 2).

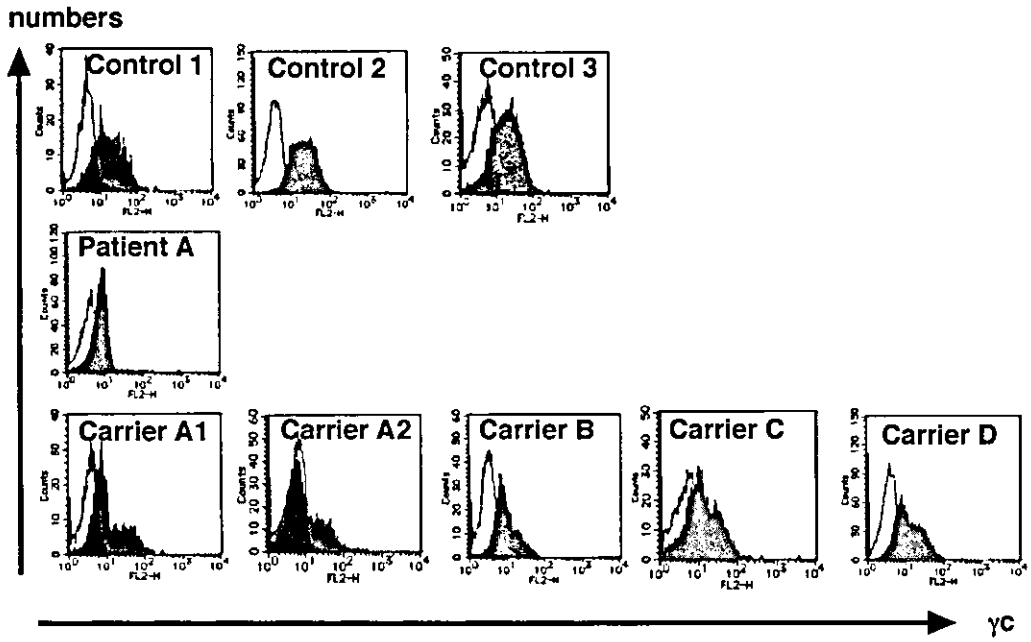

Fig 1. Flow cytometric analysis of γc expression on monocytes from an X-SCID patient and five carriers. Monocytes were gated by FSC/SSC pattern and studied for γc. Shaded area represents anti-γc mAb staining and blank area represents isotypic control Ab staining. Both the γc-positive and -negative populations were detected in all five X-SCID carriers. (Note: carriers showed double peaks.)

Table I. Data of fluorescent intensity in Fig 1.

	Median value	Geometric mean
Control 1	19·28	24·53
Control 2	15·12	20·89
Control 3	17·15	21·36
Patient A	7·64	7·95
Carrier A1	7·91	14·84
Carrier A2	6·49	13·71
Carrier B	8·43	10·87
Carrier C	11·04	17·72
Carrier D	10·18	15·45

Flow cytometric analysis of X-SCID patients after CBSCT

It was shown that all T ($CD4^+$ and $CD8^+$) and NK ($CD56^+$) cells, although some were small in cell number, possessed γc. In contrast, the majority of B ($CD20^+$) and monocytes were negative for γc (Fig 2).

Detection of the mutant γc mRNA in X-SCID carriers' monocytes

i) Size difference of γc mRNA in RT-PCR product. The mutant γc mRNA in monocytes from carrier C was clearly detected by RT-PCR. Together with the normal sized fragment (700 bp), the mutant small band excluding exons 4 and 5 (397 bp; confirmed by sequencing) was detected in her monocytes, but not in her T or B cells (Fig 3). The proportion of the mutant message was estimated as 45% by densitometric analysis (Table II).

ii) Sequencing results of γc mRNA. γc mRNAs from various types of blood cells from carriers A1, A2 and B were RT-PCR-amplified, and resultant cDNAs were directly sequenced. It was shown that the γc message of monocytes included both the mutant and wild-type sequences, whereas those from $CD3^+$ or $CD20^+$ cells possessed only the wild-type sequence (data not shown).

iii) Clonal studies. Clones including the part of γc cDNA from various types of cell from carriers A1, A2 and B were sequenced to identify the mutant or wild sequence. It was shown that the mutant clones were detected in monocytes from the three carriers (Table II). The percentage of the mutant clones from monocytes ranged from 13·2 to 34·1%. In contrast, no mutant clone was detected from their $CD3^+$, $CD20^+$ cells.

DISCUSSION

Using flow cytometric analysis, we have shown that five X-SCID carriers' monocytes consist of two populations with γc-positive and negative. We also detected the mutant γc message expressed in monocytes from four carriers. In contrast, neither T nor B cells from the carriers expressed the mutant γc message, which was consistent with previous studies of X-SCID carriers (Wengler *et al*, 1993). We also showed that two X-SCID patients with successful CBSCT persistently possessed γc-negative monocytes. This is the first report to study the expression of γc on the monocytes

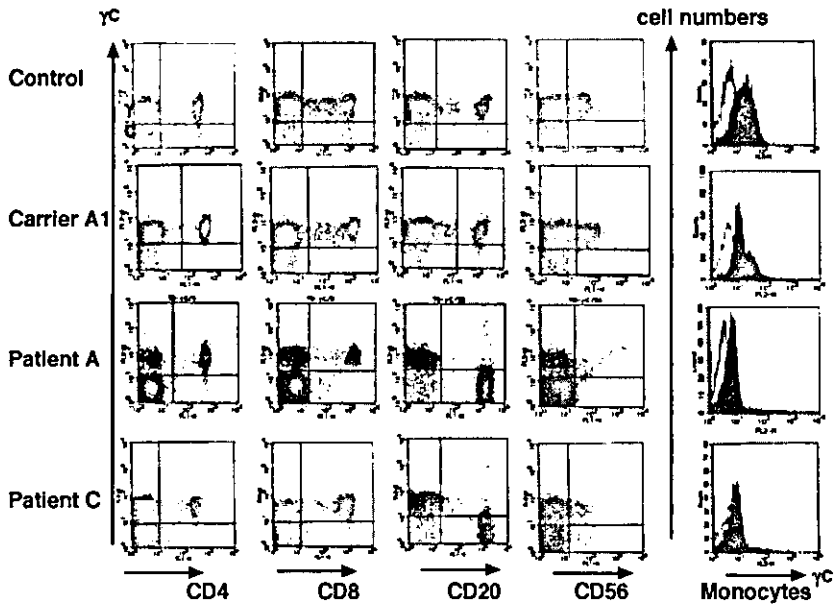

Fig 2. Flow cytometric analysis of γc expression in lymphocyte subsets and monocytes. Both lymphocytes and monocytes were gated by the FSC/SSC pattern and analysed. The results of X-SCID carrier A1 and X-SCID patients (patients A and C) 1 and 3 years after CBSCT, respectively, are shown. In the patients, most $CD4^+$, $CD8^+$ and $CD56^+$ cells show positive for γc, whereas γc is still negative for $CD20^+$ and monocytes.

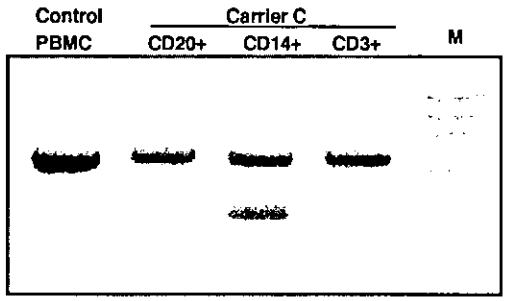

Fig 3. RT-PCR for the γc message using $CD3^+$, 14^+ and 20^+ cells from carrier C. RNAs from each separated cell were used for cDNA synthesis; then, the part of γc cDNA including the mutation was amplified as described in *Materials and methods*. The mutant γc cDNA was easily detected as a short fragment. The proportion of the mutant message was estimated as densitometer analysis. PBMC, peripheral blood mononuclear cell; M, molecular marker of ϕX174 *Hae* III digested.

Table II. Proportion (%) of the mutant γc message detected in X-SCID carriers.

	$CD3^+$	$CD20^+$	$CD14^+$
Carrier A1	0 (0/7)	0 (0/26)	28·0 (7/25)
Carrier A2	N.D.	0 (0/24)	13·2 (5/38)
Carrier B	0 (0/24)	0 (0/30)	34·1 (14/41)
Carrier C	0	0	45·0

N.D., not done. Proportion of carriers A1, A2 and B was calculated from clonal studies indicated in the parentheses. Proportion of carrier C was estimated from the result shown in Fig 3 by densitometric analysis.

from genetically diagnosed X-SCID carriers and X-SCID patients after HSCT.

γc is expressed in monocytes as well as T, B and NK cells. γc on monocytes is used to combine interleukin 2 receptor (IL-2R) with IL-2R α- and β-chain, or IL-4R with IL-4R α-chain respectively. IL-2 and IL-4 regulate the production of other cytokines, such as sIL1ra, IL-1β, IL-8, IL-10, IL-12 and TNF-α from monocytes/macrophages. Monocyte function in a SCID patient with mutant Jak3, which is a signal transduction molecule functionally coupled with γc, was reported as normal (Villa *et al*, 1996), suggesting that the signalling event via jak3 in monocytes was dispensable. In addition, IL-4 mediated signalling can be conveyed in X-SCID B cells via a γc-independent pathway (Taylor *et al*, 1997). In contrast, the role of γc in monocyte development/function *in vivo* has not been fully studied, although *in vitro* studies of IL-4-mediated effects via γc on normal monocytes were reported (Bonder *et al*, 1998, 1999). X-SCID patients show the normal number of γc-negative monocytes, however, this does not always mean that γc is dispensable molecule for monocyte development, as a significant number of γc-negative B cells are detected in X-SCID patients regardless of its important role in B-cell development. To investigate the role of γc in human monocyte development/function *in vivo*, we expected that X-SCID carriers and X-SCID patients after HSCT could be good subjects to study.

First, we were curious about the expression of γc on monocytes from X-SCID carriers. The important role of γc in B-cell development was highlighted in X-SCID carriers; no B cell with mutant γc was detected in them. Thus, to investigate the role of the disease-causing molecule in the X-chromosome *in vivo*, the evaluation of its expression in female carriers would be a more accurate method (Ariga *et al*, 1999; Yamada *et al*, 2000). Using flow cytometric analysis, we detected γc-negative monocytes in the five X-SCID carriers together with γc-positive monocytes,

suggesting that this method could be applied for X-SCID carrier screening. Two populations, however, overlapped in part because the normal γc on their monocytes expressed varied in amount. The varied γc expression was also observed in monocytes from normal individuals as the normal distribution pattern. Among normal individuals γc expression seemed to be different in amount, although we could definitely distinguish between that of the patient or carriers (Fig 1). The expression of γc on monocytes reduces during *in vitro* culture (Bonder *et al*, 1998). Thus, it may reflect the different condition of monocytes upon evaluation.

To confirm the results of flow cytometric analysis, we attempted to detect the mutant γc message from these four carriers. The direct sequencing studies of RT-PCR products from carriers A1, A2 and B were performed. We detected a mixed sequence of the normal and mutant γc messages from monocytes but not from T or B cells (data not shown). Further cloning studies confirmed that the mutant γc clones were detected from the monocytes of these carriers (13·2–34·1%; Table II). In contrast, no mutant γc cDNA clone was detected from the T or B cells, indicating that those cells with the mutant γc could not develop *in vivo* in X-SCID carriers as speculated previously (Conley *et al*, 1988). We also detected the small-sized mutant γc message from monocytes, not from T or B cells of carrier C (Fig 3, Table II). These results clearly indicated that γc molecule is not essential for monocyte development *in vivo*, which is consistent with a previous report (Wengler *et al*, 1993), which found that the random X-chromosomal inactivation pattern was detected in monocytes from obligate X-SCID carriers.

Second, we studied two X-SCID patients after CBSCT who made good clinical progress. One and 3 years after CBSCT, respectively, it was revealed that the majority of their monocytes still consisted of γc-negative cells. These cells were of recipient origin. It may suggest that without the γc molecule, monocyte/macrophage can be functional because both patients had not had any serious infectious episodes since the CBSCT.

Haddad *et al* (1999) also reported that 13/14 of monocytes from X-SCID patients were still host origin after HSCT. Recently, successful haematopoietic stem cell gene therapies for X-SCID patients have been reported (Cavazzana-Calvo *et al*, 2000). After the therapies, patients could make antigen-specific immune responses, although gene-introduced monocytes were hardly observed in them (A. Fisher, personal communication). Taken together, these results suggest that the γc molecule on monocytes is dispensable for their development and function *in vivo*; however, it remains to be defined whether γc-negative monocytes are as fully functional as γc-positive monocytes.

ACKNOWLEDGMENTS

We are grateful to Professor K. Kobayashi for the critical comment on the article. We also thank the medical staff for their excellent patient care. This work was supported by the H12-genome-003 grant from the Ministry of Health, Labour and Welfare, Japan, and the grant 13670776 from the Ministry of Education, Culture, Sports, Science and Technology, Japan.

REFERENCES

Ariga, T., Yamada, M., Wada, T., Saitoh, S. & Sakiyama, Y. (1999) Detection of lymphocytes and granulocytes expressing the mutant WASP message in carriers of Wiskott–Aldrich syndrome. *British Journal of Haematology*, **104**, 893–900.

Asao, H., Okuyama, C., Kumaki, S., Ishii, N., Tsuchiya, S., Foster, D. & Sugamura, K. (2001) The common gamma-chain is an indispensable subunit of the IL-21 receptor complex. *Journal of Immunology*, **167**, 1–5.

Bonder, C.S., Dickensheets, H.L., Finlay-Jones, J.J., Donnelly, R.P. & Hart, H. (1998) Involvement of the IL-2 receptor γ-chain (γc) in the control by IL-4 human monocytes and macrophage pro-inflammatory mediator production. *Journal of Immunology*, **160**, 4048–4056.

Bonder, C.S., Finlay-Jones, J.J. & Hart, P.H. (1999) Interleukin-4 regulation of human monocyte and macrophage interleukin-10 and interleukin-12 production. Role of a functional interleukin-2 receptor γ-chain. *Immunology*, **96**, 529–536.

Buckley, R.H., Schiff, S.E., Schiff, R.I., Markert, M.L., Williams, L.W., Roberts, J.L., Myers, L.A. & Ward, F.E. (1999) Hematopoietic stem-cell transplantation for the treatment of severe combined immunodeficiency. *New England Journal of Medicine*, **340**, 508–516.

Cao, X., Shores, E.W., Hu-Li, J., Anver, M.R., Kelsall, B.L., Russell, S.M., Drago, J., Noguchi, M., Grinberg, A., Bloom, E.T., Paul, W.E., Katz, S.I., Love, P.E. & Leonard, W.J. (1995) Defective lymphoid development in mice lacking expression of the common cytokine receptor gamma chain. *Immunity*, **2**, 223–238.

Cavazzana-Calvo, M., Hacein-Bey, S., de Saint Basile, G., Gross, F., Yvon, E., Nusbaum, P., Selz, F., Hue, C., Certain, S., Casanova, J.L., Bousso, P., Deist, F.L. & Fischer, A. (2000) Gene therapy of human severe combined immunodeficiency (SCID)-X1 disease. *Science*, **288**, 669–672.

Conley, M.E., Lavoie, A., Briggs, C., Brown, P., Guerra, C. & Puck, J.M. (1988) Nonrandom X chromosome inactivation in B cells from carriers of X-chromosome-linked severe combined immunodeficiency. *Proceedings of the National Academy of Sciences of the United States of America*, **85**, 3090–3094.

DiSanto, J.P., Muller, W., Guy-Grand, D., Fischer, A. & Rajewsky, K. (1995) Lymphoid development in mice with a targeted deletion of the interleukin 2 receptor gamma chain. *Proceedings of the National Academy of Sciences of the United States of America*, **92**, 377–381.

Haddad, E., Deist, F.L., Aucouturier, P., Cavazzana-Calvo, M., Blanche, S., De Saint Balile, G. & Fisher, A. (1999) Long-term chimerism and B-cell function after bone marrow transplantation in patients with severe combined immunodeficiency with B cells: a single-center study of 22 patients. *Blood*, **94**, 2923–2930.

Ishii, N., Takeshita, T., Tada, K., Kondo, M., Nakamura, M. & Sugamura, K. (1994) Expression of the IL-2 receptor γ chain on various populations in human peripheral blood. *International Immunology*, **6**, 1273–1277.

Kumaki, S., Ishii, N., Minegishi, M., Ohashi, Y., Hakozaki, I., Nonoyama, S., Imai, K., Morio, T., Tsuge, I., Sakiyama, Y., Miyanoshita, A., Miura, J.-I., Mayumi, M., Heike, T., Katamura, K., Takada, H., Izumi, I., Kamizono, J., Hibi, S., Sasaki, H., Kimura, M., Kikuta, A., Date, Y., Sako, M., Tanaka, H., Sano, K., Sugamura, K. & Tsuchiya, S. (2000) Characterization of the γc chain among 27 unrelated Japanese patients with X-linked immunodeficiency (X-SCID). *Human Genetics*, **107**, 406–408.

Leonard, W.J., Shores, E.W. & Love, P.E. (1995) Role of the common cytokine receptor gamma chain in cytokine signaling and lymphoid development. *Immunology Review*, **148**, 97–114.

Malek, T.R., Porter, B.O. & He, Y.-W. (1999) Multiple γc-dependent cytokines regulate T cell development. *Immunological Today*, **20**, 71–76.

Noguchi, M., Yi, H., Rosenblatt, H.M., Filipovich, A.H., Adelstein, S., Modi, W.S., McBride, O.W. & Leonard, W.J. (1993) Interleukin 2 receptor gamma chain mutation results in X-linked severe combined immunodeficiency in humans. *Cell*, **73**, 147–157.

Otsu, M., Sugamura, K. & Candotti, F. (2000) In vivo competitive studies between normal and common gamma chain-defective bone marrow cells: implications for gene therapy. *Human Gene Therapy*, **11**, 2051–2056.

Puck, J.M., Deschenes, S.M., Porter, J.C., Dutra, A.S., Brown, C.J., Willard, H. & Henthorn, F.P.S. (1993) The interleukin-2 receptor gamma chain maps to Xq13.1 and is mutated in X-linked severe com-bined immunodeficiency, SCIDX1. *Human Molecular Genetics*, **2**, 1099–1104.

Sugamura, K., Asao, H., Kondo, M., Tanaka, N., Ishiii, N., Nakamura, M. & Takeshita, T. (1995) The common gamma chain for multiple cytokine receptors. *Advance in Immunology*, **59**, 225–277.

Taylor, N., Candotti, F., Smith, S., Oakes, S.A., Jahn, T., Isakov, J., Puck, J.M., O'Shea, J.J., Weinberg, K. & Johnston, J.A. (1997) Interleukin-4 signaling in B lymphocytes from patients with X-linked severe combined immunodeficiency. *Journal of Biological Chemistry*, **272**, 7314–7319.

Villa, A., Sironi, M., Macchi, P., Matteucci, C., Notarangelo, L.D., Vezzoni, P. & Montavani, A. (1996) Monocyte function in a severe combined immunodeficient patient with a donor splice site mutation in the Jak3 gene. *Blood*, **88**, 817–823.

Wengler, G.S., Allen, R.C., Parolini, O., Smith, H. & Conley, M.E. (1993) Nonrandom X chromosome inactivation in natural killer cells from obligate carriers of X-linked severe combined immunodeficiency. *Journal of Immunology*, **150**, 700–704.

Yamada, M., Ariga, T., Kawamura, N., Yamaguchi, K., Ohtsu, M., Nelson, D.L., Kondoh, T., Kobayashi, I., Okano, M., Kobayashi, K. & Sakiyama, Y. (2000) Determination of carrier status for the Wiskott–Aldrich syndrome by flow cytometric analysis of Wiskott–Aldrich syndrome protein expression in peripheral blood mononuclear cells. *Journal of Immunology*, **165**, 1119–1122.

Selective loss of gastrointestinal mast cells and impaired immunity in PI3K-deficient mice

Taro Fukao[1], Taketo Yamada[2], Masanobu Tanabe[3], Yasuo Terauchi[4], Takayuki Ota[1], Tetsuro Takayama[1], Tomoichiro Asano[4], Tsutomu Takeuchi[3], Takashi Kadowaki[4], Jun-ichi Hata[2] and Shigeo Koyasu[1]

Published online: 19 February 2002, DOI: 10.1038/ni768

Mice that lack the p85α regulatory subunit of phosphatidylinositol-3 kinase (PI3K) are deficient in gastrointestinal and peritoneal mast cells but have dermal mast cells. Accordingly, these mice show impaired bacterial clearance in response to acute septic peritonitis and are highly susceptible to infection by the intestinal nematode *Strongyloides venezuelensis*. Systemic anaphylactic shock responses, however, are intact. We found that although reconstitution of PI3K$^{-/-}$ mice with bone marrow–derived mast cells (BMMCs) restored anti-bacterial immunity, only T helper type 2 (T_H2)-conditioned BMMCs, not "standard" BMMCs, were able to restore anti-nematode immunity. This finding highlights the importance of the T_H2 response in the control of nematode infection. Thus, PI3K likely plays an essential role in host immune responses by regulating both the development and induction of mast cells.

Mast cells are central effectors in allergic and T helper type 2 (T_H2)-mediated immune responses[1–3]. In addition, they may be critical components in the induction of innate immunity[4,5]. Activation of mast cells with immunoglobulin E (IgE)-dependent and IgE-independent agonists results in immediate release of various biological mediators, including histamine, leukotrienes, proteases, prostaglandins and cytokines[1–3]. Together, these facts suggest that mast cells can influence and mediate many of the normal and pathogenic phases of immunity.

The development of mast cells has been extensively investigated[1–3] and the regulatory mechanisms that govern mast cell development can be divided into two distinct immune phases[6,7]. First is the normal or steady-state immune phase, when resident mast cells continuously develop in a homeostatic manner; second is the pathogenic or inflammatory immune phase, when mast cells are rapidly induced in response to pathogenic invasions[6,7].

With regard to development in the absence of pathogenic invasion, mature mast cells are present in all vascularized tissues, especially at the sites of internal-external borders, such as the gastrointestinal tract and under the epithelial layer of the skin[1–3]. Mast cells are derived from hematopoietic precursors that originate in the bone marrow; unlike other hematopoietic cells, however, they leave the bone marrow as progenitors and complete their maturation after migration into peripheral tissues[1–3]. Committed mast cell progenitors have been described[8,9], but the basic developmental cues required for mast cell production have not yet been established.

The primary signal required for survival and maintenance of mast cells in peripheral tissues has been identified. Binding of stem cell factor (SCF) to its receptor c-Kit appears to be the primary event upon which mature mast cells are essentially dependent[1–3,10]. Mice with double-mutant alleles at the SCF locus (which is encoded by *Kitl*, also known as *Sl*) or at the c-Kit locus (which is encoded by *Kit*, also known as *W*) show severe mast cell deficiencies in all organs and tissues[11,12]. However, how the development of distinct populations of mast cells—which localize to different anatomical sites and play specific physiological roles[1–3]—is differentially regulated is currently unclear.

The expulsion of many intestinal parasites—including *Trichinella spilaris* and *Strongyloides venezuelensis*—requires the hyperplasia of differentiated mast cells, that is, mastocytosis in the gastrointestinal tract[13–15]. Mastocytosis is dependent on several cytokines, including interleukin 3 (IL-3), IL-4 and IL-10, which determine not only the growth, but also the phenotypes, of mast cells[7,13–18]. Because these cytokines are produced by T_H2 cells, an effective T_H2 response is critical for the induction of mastocytosis and subsequent parasite rejection[7,13,19]. Defective anti-parasitic immunity in several gene-targeted mice lacking molecules essential for successful T_H2 induction supports this[13,20,21].

[1]*Department of Microbiology and Immunology,* [2]*Department of Pathology and* [3]*Department of Tropical Medicine and Parasitology, Keio University School of Medicine, 35 Shinanomachi, Shinjuku-ku, Tokyo 160-8582, Japan.* [4]*Department of Metabolic Diseases, Graduate School of Medicine, University of Tokyo, 7-3-1 Hongo, Bunkyo-ku, Tokyo 113-8655, Japan. Correspondence should be addressed to S. K. (koyasu@sc.itc.keio.ac.jp)*

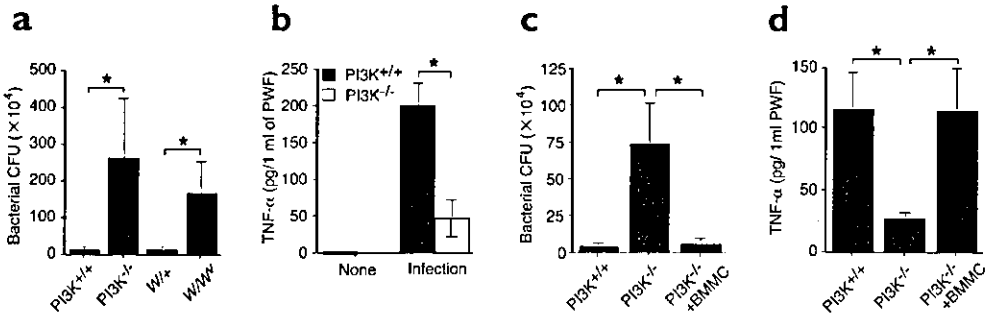

Figure 1. Impaired acute bacterial clearance in PI3K$^{-/-}$ mice. (**a**) Age- and sex-matched (female) PI3K$^{+/+}$ (n=5), PI3K$^{-/-}$ (n=5), W/+ (n=5) and W/W^{v} (n=5) mice were examined for acute septic peritonitis, bacterial dose: A_{600} 0.12 (see Methods), and the numbers of bacteria that survived in the peritoneal cavities recorded. (**b**) Immediate release of TNF-α in the peritoneum was examined in PI3K$^{+/+}$ (n=4) and PI3K$^{-/-}$ (n=4) mice (see Methods). (**c**) PI3K$^{+/+}$ (n=3), PI3K$^{-/-}$ (n=3) and peritoneal mast cell–reconstituted PI3K$^{-/-}$ mice (n=3) were examined for acute septic peritonitis, bacterial dose: A_{600} 0.10. (**d**) TNF-α in the peritoneum was examined 1 h after infection in PI3K$^{+/+}$ (n=3), PI3K$^{-/-}$ (n=3) and peritoneal mast cell–reconstituted PI3K$^{-/-}$ (n=3) mice. *P<0.05.

Phosphatidylinositol-3 kinases (PI3Ks) are lipid kinases that catalyze the conversion of phosphatidylinositol(4,5)bisphosphate (PIP_2) to PIP_3[22]. Class I_A PI3K, which consists of regulatory and catalytic subunits, is involved in multiple signal transduction cascades that regulate cell proliferation, survival and differentiation[22]. Although various receptor signaling pathways, including those mediated by FcεRI and c-Kit, can activate class I_A PI3K in mast cells[23,24], the role of class I_A PI3K in the differentiation of mast cells *in vivo* is poorly understood.

We show here the role of class I_A PI3K in the development of mast cells *in vivo* by analyzing PI3K$^{-/-}$ mice, in which the gene encoding the p85α regulatory subunit of the most abundantly expressed isozyme of class I_A PI3K[25–27] has been disrupted[28,29]. PI3K$^{-/-}$ mice were severely deficient in gastrointestinal and peritoneal mast cells, whereas dermal mast cells were found in their skin. Consistent with this phenotype, PI3K$^{-/-}$ mice were no longer resistant to acute septic peritonitis, a process generally controlled by peritoneal mast cells[4,5]. However, these mice showed strong systemic anaphylaxis[30], which indicated that functional mast cells were present at other anatomical sites. Abnormal development of peritoneal mast cells in PI3K$^{-/-}$ mice during the normal or steady-state immune phase accounted for the defective immunity to septic peritonitis, as reconstitution with bone marrow–derived mast cells (BMMCs) restored anti-bacterial immunity in PI3K$^{-/-}$ mice. In addition, impaired immunity to *S. venezuelensis* was observed in PI3K$^{-/-}$ mice. High susceptibility to *S. venezuelensis* resulted from defects in the induction of mastocytosis because reconstitution of PI3K$^{-/-}$ mice with T_H2-conditioned BMMCs, but not with standard BMMCs, restored anti-parasitic immunity; this highlighted the importance of T_H2 responses in anti-nematode immunity. Concomitantly, mesenteric lymph node cells from infected PI3K$^{-/-}$ mice produced reduced amounts of several T_H2 cytokines, which could account for the defect in mastocytosis. Taken together, our observations establish an essential role for class I_A PI3K in the development of mast cells during both the normal and pathogenic immune responses.

Results

Impaired acute bacterial clearance in PI3K$^{-/-}$ mice

PI3K$^{-/-}$ mice are highly susceptible to bacterial infections such as *Corynebacterium kutcheri*[28,29]. Although abnormal B cell differentiation in PI3K$^{-/-}$ mice has been reported[29], the high susceptibility to bacterial infection suggested an additional impairment in the innate immune systems of these mice[29].

To examine bacterial immunity in PI3K$^{-/-}$ mice, enterobacteria from the ceca of BALB/c mice were injected into the peritoneal cavities of PI3K$^{+/+}$ and PI3K$^{-/-}$ mice. After 3 h, the number of bacteria that survived in the peritoneal cavities of PI3K$^{-/-}$ mice was much higher than in PI3K$^{+/+}$ mice (**Fig. 1a**), which suggested that acute bacterial clearance was defective in PI3K$^{-/-}$ mice. Because immediate release of tumor necrosis factor-α (TNF-α) is critical to acute bacterial clearance[4,5], we examined TNF-α production in the peritoneal cavities of infected mice after 1 h of infection and found that significantly (P<0.05) lower amounts of TNF-α were released in the peritoneal cavities of PI3K$^{-/-}$compared to PI3K$^{+/+}$ mice (**Fig. 1b**).

The mast cell is a well known effector that is pivotal to a variety of allergic events[1–3]. As the source of TNF-α, these cells are also important in acute microbial clearance[4,5]. Therefore, we examined the presence of mast cells in peritoneal cavities of PI3K$^{-/-}$ mice. Flow cytometric analysis showed that the number of mast cells (FcεRI^{+}c-Kit^{+}) in the peritoneal cavities of

Table 1. Mast cell number in different anatomical sites

	Mast cells/unit[a]			Student's t-test[b]
	PI3K$^{+/+}$	PI3K$^{+/-}$	PI3K$^{-/-}$	
Peritoneum[c] (n=5)	1.34±0.26	1.28±0.32	0.32±0.12	P<0.001
Ear dermis (n=6)	122.0±13.2	102.7±18.3	78.8±13.4	P<0.001
Back dermis (n=6)	50.3±4.2	51.0±6.0	38.7±7.8	P<0.025
Stomach: mucosa	51.2±9.8	48.5±12.0	0.0±0.0	P<0.001
Stomach: submucosa	120.2±21.2	133.4±15.6	0.0±0.0	P<0.001
Stomach: muscularis (n=8)	36.8±6.3	23.5±9.1	0.0±0.0	P<0.001
Jejunum (n=8)	11.3±4.5	5.5±2.5	0.0±0.0	P<0.001
Ileum (n=8)	7.8±3.5	4.6±2.1	0.0±0.0	P<0.001
Colon (n=8)	3.8±1.6	3.4±1.1	0.0±0.0	P<0.001

[a]The unit definition for each anatomical site is described in the Methods. [b]Student's t-tests were done as +/+ *versus* –/– animals. [c]Data are presented as the mean±s.d. percentages of mast cells (FcεRI^{+}c-Kit^{+} cells) in total peritoneal cells.

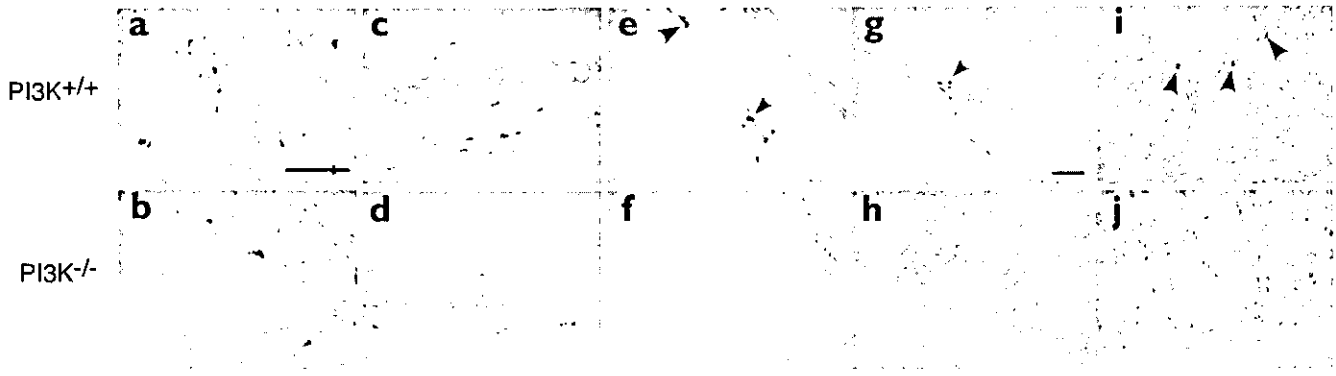

Figure 2. Selective loss of gastrointestinal mast cells in PI3K$^{-/-}$ mice. Dermal mast cells in the back (**a,b**) and ear (**c,d**) skin were detected in PI3K$^{+/+}$ (**a,c**) and PI3K$^{-/-}$ (**b,d**) mice with toluidine blue staining. The highly metachromatic cells are mast cells. Mast cells (arrows) were readily detected in the stomachs of PI3K$^{+/+}$ mice (**e**) but were absent in the stomachs of PI3K$^{-/-}$ mice (**f**). Mast cells that have chloroacetate esterase activities (red cells) were present in the stomachs (**g**) and small intestines (**i**) of PI3K$^{+/+}$ mice, but were absent in the stomachs (**h**) and small intestines (**j**) of PI3K$^{-/-}$ mice. Original magnifications: **a–f**: ×200, **g–j**: ×100. Scale bars, 100 μm. Data are representative of samples from nine (for toluidine blue staining) or six (for chloroacetate esterase staining) individual mice with similar results.

PI3K$^{-/-}$ mice were reduced in comparison to those present in PI3K$^{+/+}$ or PI3K$^{+/-}$ mice (**Table 1**).

Cultured bone marrow–derived mast cells (BMMCs) from PI3K$^{+/+}$ mice were then injected into the peritoneum of PI3K$^{-/-}$ mice in order to reconstitute peritoneal mast cells[4,5]. Injection of PI3K$^{+/+}$ BMMCs completely restored peritoneal mast cells in PI3K$^{-/-}$ mice (PI3K$^{+/+}$ 1.58±0.21%, n=3; PI3K$^{-/-}$ + BMMCs 1.74±0.20%, n=3). Subsequently, we examined the immune response to bacteria in mast cell–reconstituted PI3K$^{-/-}$ mice. In these mice, bactericidal activity and the degree of acute TNF-α release were restored to the equivalent amounts observed in PI3K$^{+/+}$ mice (**Fig. 1c,d**). It is therefore likely that the lack of peritoneal mast cells in PI3K$^{-/-}$ mice was the cause of impaired bacterial clearance in response to acute septic peritonitis[4,5].

Loss of gastrointestinal mast cells in PI3K$^{-/-}$ mice

Having observed a significant reduction in the number of peritoneal mast cells, we examined the presence of mast cells in other anatomical sites (**Fig. 2**). As assessed by toluidine blue staining, dermal mast cells were observed in the ear and dorsal skin of PI3K$^{-/-}$ mice, even though the cell density was reduced (there was a maximal ~35% reduction in the ear dermis) (**Fig. 2a–d** and **Table 1**). The distribution and number of dermal mast cells in PI3K$^{+/-}$ mice was similar to that in PI3K$^{+/+}$ mice (**Table 1**). The degree of purple coloration of PI3K$^{+/+}$, PI3K$^{+/-}$ and PI3K$^{-/-}$ dermal mast cells stained with toluidine blue was indistinguishable (**Fig. 2a–d** and data not shown). This suggested that the disruption of PI3K had little effect on the generation of glycosaminoglycans, polyanionic glycans that alter the color of toluidine blue (metachromasia)[31,32]. Subsequently, the gastrointestinal tract was tested for the presence of mast cells. Although mast cells (positive for toluidine blue, alcian blue–safranin staining or chloroacetate esterase activity[22]) were readily detected in the mucosal, submucosal and muscular layers of the stomach of PI3K$^{+/+}$ mice (**Fig. 2e,g** and **Table 1**), no mast cells were observed in the stomach of PI3K$^{-/-}$ mice (**Fig. 2f,h** and **Table 1**). Again, the distribution and number of gastric mast cells in PI3K$^{+/-}$ mice were almost identical to those of PI3K$^{+/+}$ mice (**Table 1**). Next, intestinal mast cells were examined in the jejunum, ileum and colon of the PI3K$^{-/-}$ mice (**Fig. 2i,j** and **Table 1**). Mast cells were completely absent in the intestines of PI3K$^{-/-}$ mice. These results collectively indicate that PI3K is essential for the normal homeostatic production of gastrointestinal mast cells, but dispensable for dermal mast cell production.

Residual mast cells in PI3K$^{-/-}$ mice

We then questioned whether residual mast cells in PI3K$^{-/-}$ mice were functionally competent. To address this issue, IgE-dependent passive systemic anaphylaxis (PSA)[33] was induced in PI3K$^{+/+}$ and PI3K$^{-/-}$ mice and in WBB6F1 *W/W^{v}* (referred to hereafter as *W/W^{v}*) mice, a strain of mice that genetically lack every type of mast cell[11,12]. Although *W/W^{v}* mice actively sensitized with protein antigens can

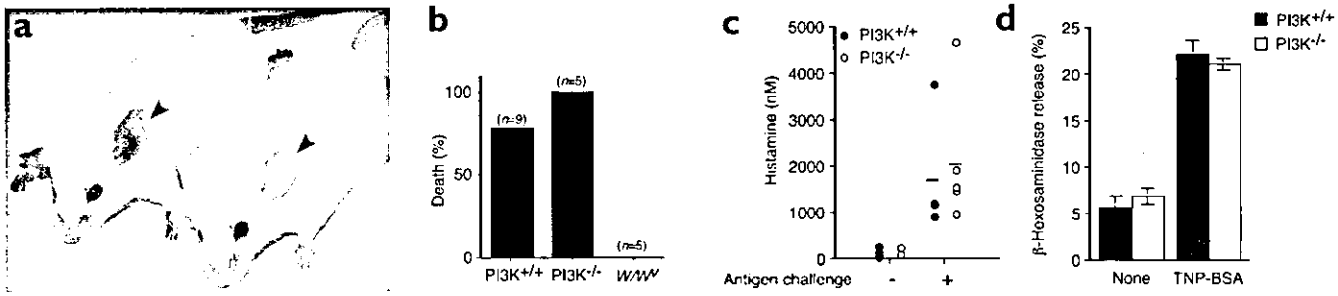

Figure 3. IgE-dependent passive systemic anaphylaxis in PI3K$^{-/-}$ mice. (**a**) Upon TNP-BSA challenge, injected Evans blue dye was extravasated in the ear of PI3K$^{-/-}$ mice (left) but not in *W/W^{v}* (right) mice. (**b**) Anaphylactic shock–induced death within 30 min of antigen challenge was observed in PI3K$^{+/+}$ (n=9) and PI3K$^{-/-}$ (n=5) mice but not in *W/W^{v}* mice (n=5). (**c**) IgE-dependent PSA was induced (see Methods) and plasma histamine concentration in PI3K$^{+/+}$ and PI3K$^{-/-}$ mice was measured (see Methods). (**d**) Degranulation of β-hexosaminidase from PI3K$^{+/+}$ and PI3K$^{-/-}$ BMMCs. Data are from two independent experiments that gave consistent results.

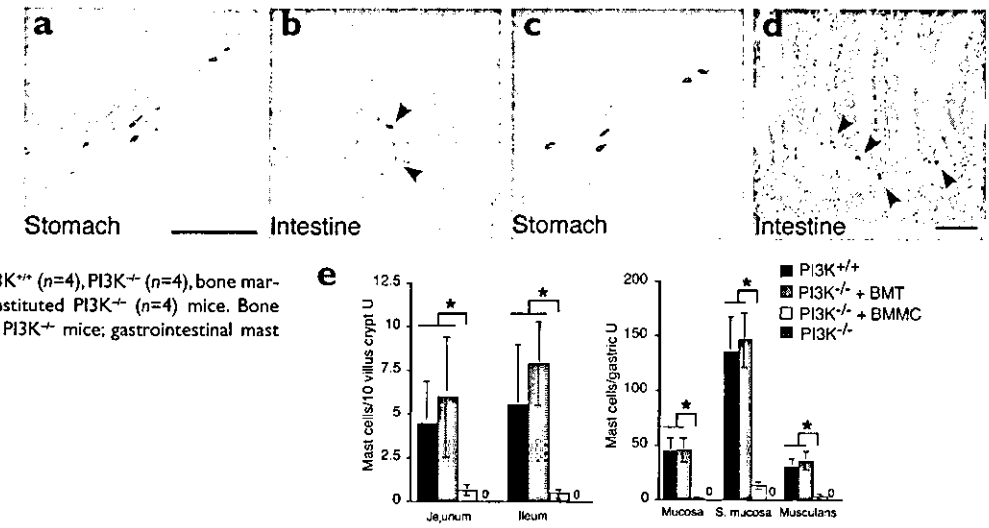

Figure 4. Gastrointestinal mast cells were restored in PI3K$^{-/-}$ mice by bone marrow transplantation. Tissues from the gastrointestinal tracts of PI3K$^{-/-}$ mice transplanted with wild-type (BALB/c mice) bone marrow were stained with toluidine blue (**a,b**), alcian blue–safranin (**c**) and for chloroacetate esterase activity (**d**). Mast cells were readily detected in the stomach (**a,c**) and small intestine (**b,d**) of PI3K$^{-/-}$ mice 12 weeks after bone marrow transplantion. Original magnification: **a–c**: ×200, **d**: ×100. Scale bars, 100 μm. (**e**) The number of gastrointestinal mast cells in PI3K$^{+/+}$ (n=4), PI3K$^{-/-}$ (n=4), bone marrow–transferred PI3K$^{-/-}$ (n=4) and BMMC-reconstituted PI3K$^{-/-}$ (n=4) mice. Bone marrow transplantion (BMT) was done on four PI3K$^{-/-}$ mice; gastrointestinal mast cells were restored in all animals. *P<0.05.

induce active fatal anaphylaxis[34,35], no anaphylactic shock is induced by direct ligation of FcεRI in the absence of antigen immunization[35,36]. This indicates that the latter reaction requires mast cells. Strong anaphylactic shock with increased vascular permeability and a high death rate were observed in both PI3K$^{-/-}$ mice and PI3K$^{+/+}$ mice (**Fig. 3a,b**). In contrast, such severe shock was not observed in *W/W^{v}* mice (**Fig. 3a,b**), in agreement with published data[35,36]. The plasma histamine concentration promptly increased after PSA and was quantitatively identical in PI3K$^{+/+}$ and PI3K$^{-/-}$ mice[33] (**Fig. 3c**). In addition, no difference in the degree of FcεRI-mediated degranulation in PI3K$^{+/+}$ and PI3K$^{-/-}$ BMMCs was observed (**Fig. 3d**). This indicated that the disruption of PI3K does not affect FcεRI-mediated degranulation, as has been reported[37]. These data indicate that residual mast cells in PI3K$^{-/-}$ mice can induce IgE-associated allergic reactions and that the production of granular contents in, and degranulation by, mast cells are not affected by the disruption of PI3K.

Defects in myeloid cells in PI3K$^{-/-}$ mice

As shown above, the reduced numbers of peritoneal mast cells in PI3K$^{-/-}$ mice were corrected by reconstitution with wild-type BMMCs. This indicated that the environmental condition for the maturation and survival of mast cell progenitors in the peritoneal cavity of PI3K$^{-/-}$ mice was intact. We then investigated whether the defective production of gastrointestinal and peritoneal mast cells in PI3K$^{-/-}$ mice was due to cell-autonomous impairment. We transplanted wild-type bone marrow cells and BMMCs[38] into PI3K$^{-/-}$ mice. Bone marrow transplantation completely restored mast cells in the stomachs and small intestines of PI3K$^{-/-}$ mice (**Fig. 4**). Although gastrointestinal mast cells were detectable in BMMC-reconstituted PI3K$^{-/-}$ mice, the restoration was only partial, as the numbers of mast cells were low compared to in PI3K$^{+/+}$ mice (**Fig. 4e**). Complete restoration of mast cells in PI3K$^{-/-}$ mice by bone marrow transplantion indicated that the production of mast cell progenitors did not

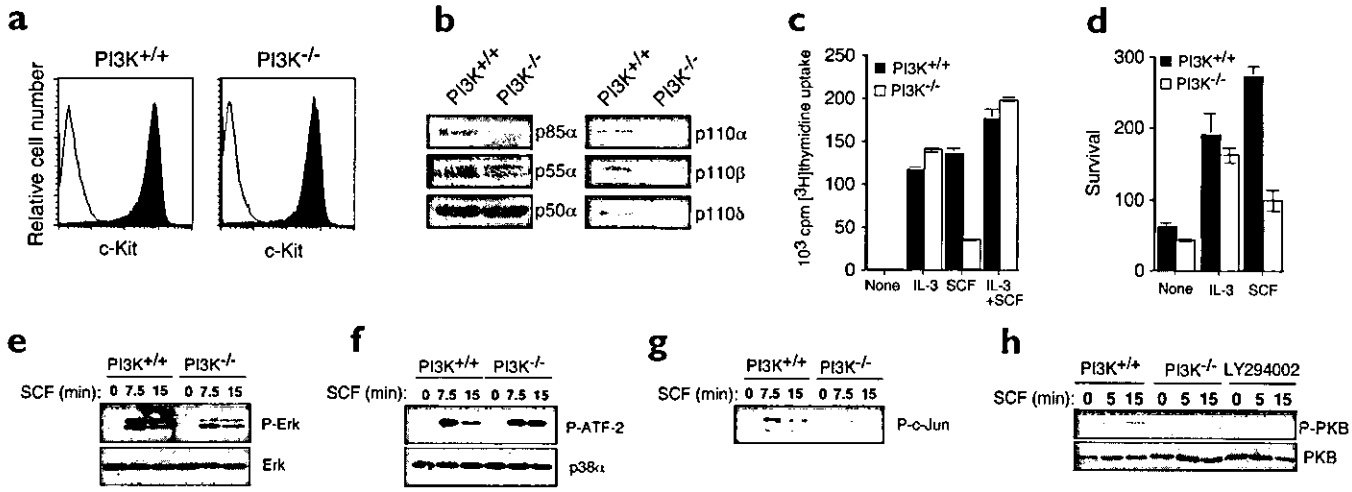

Figure 5. Defective SCF-induced proliferation in PI3K$^{-/-}$ BMMCs. (**a**) Expression of c-Kit on the surfaces of PI3K$^{+/+}$ and PI3K$^{-/-}$ BMMCs. (**b**) PI3K$^{+/+}$ and PI3K$^{-/-}$ BMMCs were examined for the expression of class I_A PI3K subunits by immunoblotting. (**c**) Proliferation of PI3K$^{+/+}$ and PI3K$^{-/-}$ BMMCs in response to IL-3 (10 ng/ml), SCF (200 ng/ml) or both was examined. Data show [^{3}H]thymidine uptake by BMMCs during 24–42 h of culture and are representative of three independent experiments that gave similar results. (**d**) Survival of PI3K$^{+/+}$ and PI3K$^{-/-}$ BMMCs 3 days after the withdrawal of IL-3 was tested in the presence or absence of IL-3 (10 ng/ml) or SCF (200 ng/ml) by trypan blue exclusion assay. Data are representative of three independent experiments that gave consistent results. The activation of Erk (**e**), p38 (**f**), Jnk (**g**) and PKB (**h**) pathways in response to SCF was examined. After 6 h of IL-3 deprivation in 0.5% FCS medium, PI3K$^{+/+}$, PI3K$^{-/-}$ and LY294002-treated (10 μM) PI3K$^{+/+}$ BMMCs were incubated with SCF (200 ng/ml) in 0.5% FCS medium for the indicated times. Kinase assays and immunoblotting were then done.

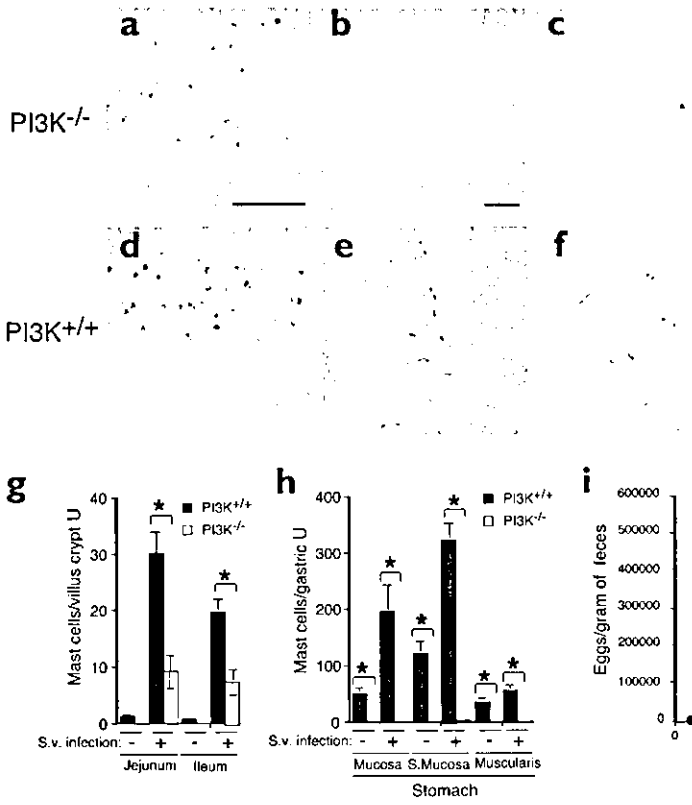

Figure 6. Modest mastocytosis and delayed expulsion of adult worms in PI3K$^{-/-}$ mice infected with *S. venezuelensis*. (**a–f**) Modest numbers of mast cells (red) were observed in the jejunum (**a**) of PI3K$^{-/-}$ mice that had been infected with *S. venezuelensis* compared with in PI3K$^{+/+}$ mice (**d**). Twelve days after infection with *S. venezuelensis*, large numbers of chloroacetate esterase–positive mast cell progenitors (**e**) and toluidine blue–positive mast cells (**f**) also appeared in the gastric submucosal layer of PI3K$^{+/+}$ mice (**e,f**) but not in PI3K$^{-/-}$ mice (**b,c**). Original magnification: **a,d**: ×200, **b,c,e,f**: ×100. Scale bars, 100 μm. Mast cells in the small intestine (**g**) and stomach (**h**) of PI3K$^{+/+}$ (n=4) or PI3K$^{-/-}$ (n=4) mice infected with *S. venezuelensis* (S.v) were counted 12 days after infection. Mast cells were identified as cells with chloroacetate esterase activity (small intestine) or metachromatic cells by toluidine blue staining (stomach). Mast cells per villus crypt unit (U)[8] (small intestine) or gastric unit (stomach) were counted. (**i**) The production of parasite eggs in the feces of PI3K$^{+/+}$ (n=5) and PI3K$^{-/-}$ (n=5) mice. (**j**) The numbers of adult worms per small intestine on day 13 of infection. Data are representative of two independent experiments that gave similar results. *P<0.05, **P<0.01.

require PI3K expression in developmental environments. This finding, together with the fact that peritoneal mast cells were completely reconstituted by injection of BMMCs, strongly suggests that the lack of peritoneal mast cells is due to cell-autonomous impairments. However, partial restoration of gastrointestinal mast cells in PI3K$^{-/-}$ mice by BMMC reconstitution points to the possible involvement of environmental defects in the impaired development of gastrointestinal mast cells.

Impaired c-Kit signaling in PI3K$^{-/-}$ BMMCs

We analyzed BMMCs from PI3K$^{-/-}$ mice to determine the molecular basis of the cell-autonomous defects that resulted from the disruption of PI3K. PI3K$^{-/-}$ BMMCs grew normally in IL-3–supplemented medium (data not shown) and expressed high amounts of FcεRI (data not shown) and c-Kit (**Fig. 5a**) on their cell surfaces[1–3]. The expression of the molecules that make up class I$_A$ PI3K[22] in PI3K$^{-/-}$ BMMCs were then examined by immunoblotting (**Fig. 5b**). Alternative splicing forms of p85α (p55α and p50α) are expressed more abundantly and may compensate for the function of p85α in certain cell types such as T cells and adipocytes in PI3K$^{-/-}$ mice[28,29]. However, the amounts of such isoforms were not increased in PI3K$^{-/-}$ BMMCs (**Fig. 5b**). We then measured the amounts of three catalytic subunits of class I$_A$ PI3K, p110α, p110β and p110δ[22], and found a marked reduction in the amount of p110α but normal expression of the other two molecules in PI3K$^{-/-}$ BMMCs (**Fig. 5b**).

Next, we examined the survival rate and proliferative ability of PI3K$^{-/-}$ BMMCs in response to IL-3 and SCF, which are essential factors in mast cell differentiation and survival[1–3,10,39,40]. Although IL-3–mediated survival and proliferation were unaffected in PI3K$^{-/-}$ BMMCs (**Fig. 5c,d**), PI3K$^{-/-}$ BMMCs showed impaired proliferation in response to SCF (**Fig. 5c**). However, SCF-mediated survival of PI3K$^{-/-}$ BMMCs was little affected, as almost 100% of cells were recovered after 3 days in SCF-supplemented culture, despite the low proliferative response (**Fig. 5d**). These results indicated that the class I$_A$ PI3K signaling pathway is important for SCF-induced proliferation of mast cells, but is dispensable for IL-3 responsiveness. The synergistic effect of SCF on IL-3–induced proliferation was intact in PI3K$^{-/-}$ BMMCs (**Fig. 5c**), which suggested that other signal transduction pathways are activated downstream of c-Kit in PI3K$^{-/-}$ BMMCs.

To identify why SCF-mediated proliferation was defective in PI3K$^{-/-}$ BMMCs, we investigated the activation of signaling molecules in PI3K$^{-/-}$ and PI3K$^{+/+}$ BMMCs downstream of c-Kit. SCF-induced activation of extracellular signal–regulated kinase (Erk)[41], as determined by phosphorylation of Erk, was slightly decreased in PI3K$^{-/-}$compared to PI3K$^{+/+}$ BMMCs (**Fig. 5e**). Although p38 activity[42] as measured by phosphorylation of ATF-2, was little affected at the early phase of activation, but was higher in PI3K$^{-/-}$ BMMCs than in PI3K$^{+/+}$ BMMCs at 15 min (**Fig. 5f**). We also found that c-Jun NH$_2$-terminal kinase (Jnk) was weakly activated in PI3K$^{-/-}$ BMMCs, whereas it was highly activated in PI3K$^{+/+}$ BMMCs in response to SCF[43] (**Fig. 5g**). Densitometric analysis showed that the peak activity of Jnk in PI3K$^{-/-}$ BMMCs was ~40% of wild-type amounts. Because SCF-induced Jnk activation is essential for the proliferation of mast cells[24], impaired Jnk activation in PI3K$^{-/-}$ BMMCs probably accounts for the defective mitogenic capacity of PI3K$^{-/-}$ BMMCs in response to SCF. The effects of the altered activation profiles of Erk and p38 in PI3K$^{-/-}$ BMMCs are unknown at present. Because protein kinase B (PKB, also known as Akt) activation depends on PI3K[44], it was expected that PKB activation would be decreased in PI3K$^{-/-}$ BMMCs. However, activation of PKB in response to SCF was readily observed in PI3K$^{-/-}$ BMMCs, although activation was slightly lower than in wild-type BMMCs (**Fig. 5h**, peak intensity in PI3K$^{-/-}$ BMMCs was

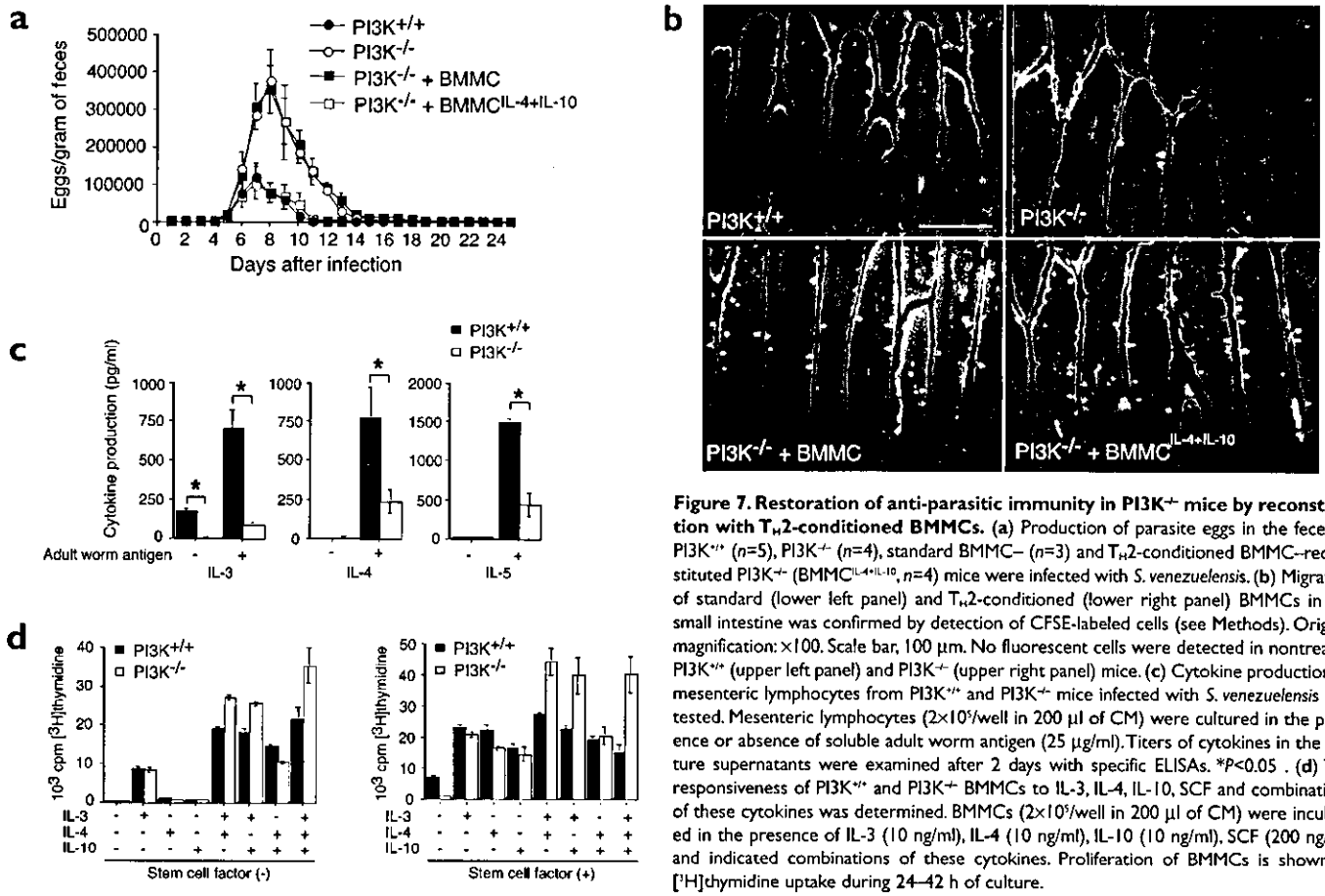

Figure 7. Restoration of anti-parasitic immunity in PI3K$^{-/-}$ mice by reconstitution with T_H2-conditioned BMMCs. (**a**) Production of parasite eggs in the feces of PI3K$^{+/+}$ (n=5), PI3K$^{-/-}$ (n=4), standard BMMC– (n=3) and T_H2-conditioned BMMC–reconstituted PI3K$^{-/-}$ (BMMC$^{IL-4+IL-10}$, n=4) mice were infected with *S. venezuelensis*. (**b**) Migration of standard (lower left panel) and T_H2-conditioned (lower right panel) BMMCs in the small intestine was confirmed by detection of CFSE-labeled cells (see Methods). Original magnification: ×100. Scale bar, 100 μm. No fluorescent cells were detected in nontreated PI3K$^{+/+}$ (upper left panel) and PI3K$^{-/-}$ (upper right panel) mice. (**c**) Cytokine production by mesenteric lymphocytes from PI3K$^{+/+}$ and PI3K$^{-/-}$ mice infected with *S. venezuelensis* was tested. Mesenteric lymphocytes (2×10^5/well in 200 μl of CM) were cultured in the presence or absence of soluble adult worm antigen (25 μg/ml). Titers of cytokines in the culture supernatants were examined after 2 days with specific ELISAs. *P<0.05 . (**d**) The responsiveness of PI3K$^{+/+}$ and PI3K$^{-/-}$ BMMCs to IL-3, IL-4, IL-10, SCF and combinations of these cytokines was determined. BMMCs (2×10^5/well in 200 μl of CM) were incubated in the presence of IL-3 (10 ng/ml), IL-4 (10 ng/ml), IL-10 (10 ng/ml), SCF (200 ng/ml) and indicated combinations of these cytokines. Proliferation of BMMCs is shown as [^{3}H]thymidine uptake during 24–42 h of culture.

~70% that of wild-type cells). This was consistent with their high survival rate in response to SCF (**Fig. 5d**).

Mastocytosis in PI3K$^{-/-}$ mice

Infection by intestinal nematodes induces extensive mastocytosis in the gastrointestinal tracts of rodents and such mastocytosis is critical for the expulsion of parasites[13,14,45–47]. To examine whether nematode-induced mastocytosis occurs in the gastrointestinal tracts of PI3K$^{-/-}$ mice, PI3K$^{+/+}$ and PI3K$^{-/-}$ mice were infected with an intestinal nematode *S. venezuelensis*[14,18,45,48,49] (**Fig. 6**). Inoculation with infective larvae (L3) of *S. venezuelensis* induced mucosal mastocytosis[14,18,45,48,49] in the jejunum and ileum of PI3K$^{-/-}$ mice (**Fig. 6a** and data not shown), although induction was modest compared with that in PI3K$^{+/+}$ mice (**Fig. 6a,d,g**). In contrast, the number of mast cells that appeared in the stomach was markedly different between PI3K$^{+/+}$ and PI3K$^{-/-}$ mice. Although a large number of mast cells (with metachromasy or chloroacetate esterase activity) were observed in the gastric submucosal layer of PI3K$^{+/+}$ mice after infection with *S. venezuelensis* (**Fig. 6e,f,h**), such mast cells were barely detectable in the stomachs of PI3K$^{-/-}$ mice (**Fig. 6b,c,h**). These results indicate that certain types of mast cells are inducible by nematode infection in the small intestine of PI3K$^{-/-}$ mice, but that PI3K is indispensable for the induction of gastric mast cells under the same condition.

Impaired immunity to *S. venezuelensis* in PI3K$^{-/-}$ mice

We also assessed immunity to *S. venezuelensis* by monitoring production of the parasite eggs in the feces of infected mice[13,14,45,48]. In this model, the number of eggs excreted in the feces is an indication of active parasitism by adult worms in the small intestine[14,44]. Although egg production in PI3K$^{+/+}$ mice became undetectable by day 11 of infection, the excretion of parasites' eggs by PI3K$^{-/-}$ mice lasted until day 22 of infection, which showed a delayed expulsion of adult worms by PI3K$^{-/-}$ mice (**Fig. 6i**). Delayed rejection of the parasites was also shown by directly counting the number of adult worms in the small intestine at day 13 of infection[44] (**Fig. 6j**). In addition, PI3K$^{-/-}$ mice showed production of ~fourfold more eggs than PI3K$^{+/+}$ mice at the peak of infection (**Fig. 6i**, PI3K$^{+/+}$ on day 7 compared to PI3K$^{-/-}$ on day 8). Taken together, these data indicate defective gastrointestinal immunity to intestinal parasites in PI3K$^{-/-}$ mice.

Restoring immunity with T_H2-conditioned BMMCs

To confirm that impaired gastrointestinal mastocytosis accounts for the defective immunity to *S. venezuelensis* in PI3K$^{-/-}$ mice[45,48], we intravenously injected cultured mast cells into PI3K$^{-/-}$ mice infected with *S. venezuelensis* on days 3, 5 and 7 after infection, to reconstitute mast cells in their gastrointestinal tracts. Immune responses were determined by measuring parasite egg production in feces, as described above. In this experiment, we prepared two types of mast cells, either "standard" PI3K$^{+/+}$ BMMCs (cultured in IL-3–supplemented medium) or T_H2-conditioned PI3K$^{+/+}$ BMMCs (grown in IL-4 and IL-10–supplemented medium during the final 3 days of cultivation). Standard BMMCs acquire a phenotype that resembles intestinal mast cells, as judged by the appearance of granular contents when grown in the presence of IL-4 and IL-10[15,50–52]. PI3K$^{-/-}$

mice reconstituted with standard BMMCs still showed impaired immunity to *S. venezuelensis*, as shown by the number of parasite eggs at the peak of infection and the number of days required to expel the parasites, which remained unchanged compared with untreated PI3K$^{-/-}$ mice (**Fig. 7a**). In contrast, reconstitution with T_H2-conditioned BMMCs quickly restored anti-parasitic immunity in PI3K$^{-/-}$ mice. The number of eggs produced at the peak of infection decreased to the amount observed in PI3K$^{+/+}$ mice. In addition, the time required to expel the parasites was reduced by reconstitution of PI3K$^{-/-}$ mice with T_H2-conditioned BMMCs (**Fig. 7a**). At day 12 of infection in one experiment, we also found a marked reduction of adult worms in PI3K$^{-/-}$ mice reconstituted with T_H2-conditioned BMMCs compared with untreated or normal BMMC–reconstituted PI3K$^{-/-}$ mice (data not shown). No differences in the numbers of transferred mast cells that reached the small intestine were observed between standard and T_H2-conditioned BMMCs, which suggested that the migratory capacities of these two types of mast cells are almost identical (**Fig. 7b**). These findings indicate that impaired immunity against infection with *S. venezuelensis* in PI3K$^{-/-}$ mice is due to the defective production of well differentiated mast cells at the site of infection, the gastrointestinal tract.

Production of cytokines by PI3K$^{-/-}$ lymphocytes

Multiple cytokines are involved in the production of mast cells in the pathogenic immune phase of parasite infection[7,16,19]. Because IL-3 is required for persistent intestinal mastocytosis in response to infection by *S. venezuelensis*[18,45] and mesenteric lymphocytes are an important source of this cytokine[17,19], we examined IL-3 production by mesenteric lymphocytes from PI3K$^{+/+}$ and PI3K$^{-/-}$ mice infected with *S. venezuelensis*. Mesenteric lymphocytes from PI3K$^{+/+}$ mice constitutively produced IL-3, which was further increased when stimulated with soluble adult worm antigen (**Fig. 7c**). However, constitutive production of IL-3 was not observed in the culture of mesenteric lymphocytes from PI3K$^{-/-}$ mice without exogenous antigen (**Fig. 7c**), and adult worm antigen-dependent production of IL-3 by lymphocytes from PI3K$^{-/-}$ mice was less than in PI3K$^{+/+}$ mice (**Fig. 7c**). Thus, lower production of IL-3 may account for the defective mastocytosis in PI3K$^{-/-}$ mice. In addition, we found that the production of other T_H2 cytokines, IL-4 and IL-5, by PI3K$^{-/-}$ mesenteric lymphocytes was also significantly reduced compared to that produced by PI3K$^{+/+}$ mesenteric lymphocytes (**Fig. 7c**, $P<0.05$). Because T_H2 cytokines are essential modulators of mast cell differentiation[7], impairment in the production of such cytokines may affect the differentiation of mast cells in the gastrointestinal tract of PI3K$^{-/-}$ mice. Nonetheless, responsiveness to these cytokines is not affected by disruption of PI3K because PI3K$^{-/-}$ BMMCs could proliferate in response to various combinations of IL-3, IL-4, IL-10 and SCF (**Fig. 7d**).

Discussion

We have shown here that the expression of the class I_A PI3K was required for the development of gastrointestinal and peritoneal mast cells, but not for development of dermal mast cells. PI3K$^{-/-}$ mice that lack gastrointestinal and peritoneal mast cells are capable of strong anaphylactic shock, but show impaired immunity to bacterial infection; both characteristics are largely mast cell–dependent immunological responses[4,5,30,33]. These results show the functional distinction between mast cells present in different anatomical sites.

PI3K$^{-/-}$ mice produced only low amounts of TNF-α in peritoneum and were unable to control acute septic peritonitis. Reconstitution of peritoneal mast cells by BMMC transfer completely restored rapid release of TNF-α and bacterial clearance in PI3K$^{-/-}$ mice. The lack of gastrointestinal mast cells also resulted in impaired intestinal anti-nematode immunity. This result supports the hypothesis that a deficiency in the production of mast cells, presumably at the site of infection (the small intestine), is the cause of the defective immunity to gastrointestinal nematode infection[13,14,45,48]. In contrast to the anti-bacterial immunity, transfer of standard BMMCs cultured in IL-3–supplemented medium was insufficient to induce the recovery of anti-nematode immunity, even though injected mast cells were readily detected in the small intestine. This result is consistent with a published report, in which repetitive injections of BMMCs did not rescue *W/W^v* mice from severe strongyloidosis, as characterized by delayed nematode rejection[53]. As shown here, transfer of T_H2-conditioned BMMCs successfully reconstituted anti-nematode immunity in PI3K$^{-/-}$ mice.

There are several possible explanations for why T_H2-conditioned, but not standard, BMMCs are able to restore immunity to intestinal parasites in PI3K$^{-/-}$ mice. One possibility is the phenotypic differences observed between standard and T_H2-conditioned BMMCs. Standard BMMCs generated in cultures supplemented with IL-3 alone are considered immature; this is based on their lack of associated protease expression[15]. However, when cultured in the presence of the T_H2 cytokines IL-4 and IL-10[7,50–52], standard BMMCs express serine proteases such as mast cell protease 1 (MCP1) and MCP2. T_H2-conditioned BMMCs thus resemble intestinal mucosal mast cells observed in the small intestine of mice infected with nematodes[15,46,50–52]. Mice that genetically lack MCP1 are unable to control infection with *Tricinella spilaris*, even though strong mastocytosis is observed in these mice, which provides direct evidence for the essential role of MCP1 in immunity to intestinal nematodes[47]. The T_H2 response is thus important for the induction of MCPs in mast cells in anti-nematode immunity. The transfer experiments we used here will be a useful tool with which to determine the relative role of mast cells in several nematode infections in mice that do not undergo mastocytosis, such as *W/W^v* and IL-3–deficient mice[45,53].

The immunodeficiency of PI3K$^{-/-}$ mice was observed with two different types of infections: acute septic peritonitis and infection by *S. venezuelensis*. We have also provided evidence that impaired production of mast cells causes the defective immune response to both infections. However, we should distinguish between the pathways that regulate the development of each population of mast cells in these two distinct infections. Impaired immunity to acute peritonitis was due to a lack of resident peritoneal mast cells, which resulted from developmental defects in the normal or steady-state immune phase. On the other hand, delayed expulsion of *S. venezuelensis* was due to impaired mastocytosis, which resulted from developmental defects in the pathogenic immune phase.

Impaired c-Kit signaling in PI3K$^{-/-}$ BMMCs provides a possible explanation for the lack of gastrointestinal and peritoneal mast cells in PI3K$^{-/-}$ mice and further emphasizes the role of class I_A PI3K in the normal or steady-state immune phase. At the molecular level, we found that Jnk activation in response to SCF was severely impaired in PI3K$^{-/-}$ BMMCs. As SCF-induced proliferation of mast cells requires Jnk activity[24], it is probable that such impairment in Jnk activation results in defective mitogenic capacity in PI3K$^{-/-}$ BMMCs. In c-Kit signaling, PI3K functions as an essential activator of Rac1, which induces the Jnk cascade[24]. Although we currently have no data on the SCF-induced activation of Rac1 in PI3K$^{-/-}$ BMMCs, the above mechanism may link defective Jnk activation and impaired proliferation in PI3K$^{-/-}$ BMMCs in response to SCF.

The SCF–c-Kit system is required for mast cell development because *W/W*^{v} and *Sl/Sl*^{d} mice (which are c-Kit– and SCF-deficient, respectively) are severely deficient in all types of mast cells[10–12]. These mice also show impaired melanogenesis and a severe anemic phenotype[10]. Although PI3K$^{-/-}$ mice are deficient in gastrointestinal and peritoneal mast cells, several types of mast cells are normally present and functionally competent in PI3K$^{-/-}$ mice, despite defective c-Kit–mediated signaling. In addition, PI3K$^{-/-}$ mice on a C57BL/6 genetic background show normal coat color, which suggests that the development of melanocytes is not affected by the lack of p85α (data not shown). In addition, PI3K$^{-/-}$ mice show no impairment of steady-state hematopoiesis (data not shown). Mice with a mutation in the binding site for the p85α subunit of PI3K in the gene encoding c-Kit have now been generated[54]. These mice have severely reduced numbers of peritoneal mast cells but show normal development of dermal mast cells. Like PI3K$^{-/-}$ mice, the c-Kit–deficient mice show no pigment deficiency or impairment of steady-state hematopoiesis; these data are consistent with our observations and support our speculation that defective c-Kit–mediated signaling plays a role in the site-selective loss of mast cells in PI3K$^{-/-}$ mice.

Dermal mast cells develop in PI3K$^{-/-}$ mice. The overlapping and/or synergistic effects of IL-3 and SCF in mast cell development and function have been demonstrated[45]. In addition, several cytokines, including IL-4 and IL-9, along with SCF and IL-3 have major effects on mast cell development[55,56]. Conservation of c-Kit–mediated signaling pathways involved in the synergistic effect of SCF on IL-3–induced proliferation in PI3K$^{-/-}$ mice suggests that the normal appearance of dermal mast cells may result from the combined effects of SCF and other such cytokines. In contrast, the role of SCF may be more important in the development of gastrointestinal and peritoneal mast cells. In this regard, we found that the level of SCF mRNA in the gastrointestinal tract was almost identical to, or possibly even higher than, that in dermis (data not shown). Despite this, the relative number of mast cells present in the gastrointestinal tract is lower than those in the dermis during the normal or steady-state immune phase. This suggests the presence of other factors that, together with SCF, support the development and survival of dermal mast cells. Such factors may be absent or present at lower amounts in the gastrointestinal tract. It is thus possible that impaired c-Kit signaling results in a more severe deficiency of mast cells in PI3K$^{-/-}$ mice at sites in which mast cell development is more dependent on SCF.

PI3K is also essential for the development of mast cells during the pathogenic immune phase, as shown by the severe defects in mastocytosis observed during infection with *S. venezuelensis* in PI3K$^{-/-}$ mice. However, the mechanisms that lead to this phenomenon are probably different to those that cause abnormal production of mast cells during the normal immune phase. Impaired IL-3 production by mesenteric lymphocytes in PI3K$^{-/-}$ mice seemed to be the main defect that led to modest mastocytosis during parasitic infection. This idea is based on data showing that mastocytosis in response to *S. venezuelensis* infection is impaired in IL-3–deficient and IL-3 hyporesponsive mice[18,45]. In addition, production of other cytokines related to the T_H2 response of parasite-specific mesenteric lymphocytes was abrogated in PI3K$^{-/-}$ mice. As well as impaired IL-3 generation, decreased production of other T_H2 cytokines may influence mastocytosis in both a quantitative and qualitative manner, resulting in the delayed rejection of intestinal nematodes by PI3K$^{-/-}$ mice. Because these cytokines, as well as IL-3, are produced by antigen-specific T_H2 cells[7,13], it is likely that induction of nematode-reactive T_H2 cells is severely blocked in PI3K$^{-/-}$ mice. We also found hyperexpression of IL-12 by dendritic cells in response to microbial stimuli and an enhanced T_H1 response in PI3K$^{-/-}$ mice (T. F. *et al.* unpublished data). This is consistent with a report that systemic administration of IL-12 prevents anti-nematode immunity[57]. We thus conclude that impaired production of T_H2 cytokines in PI3K$^{-/-}$ mice is due to defective skewing toward the T_H2 response during nematode infection.

Our study demonstrated the role of class I_A PI3K in mast cell development and in immune responses associated with mast cells. Although class I_A PI3K is essential for the production of mast cells in the normal and pathogenic immune phases, class I_A PI3K functions differently during these distinct phases. Class I_A PI3K plays a key role in the production of gastrointestinal and peritoneal mast cells during the normal immune phase. At this stage, class I_A PI3K may function as a critical mediator of c-Kit signaling in mast cells, supporting SCF-dependent mast cell proliferation in the gastrointestinal tract and peritoneal cavity. On the other hand, class I_A PI3K also acts as modulator of immune responses and drives persistent T_H2 responses during parasitic infection. Effective T_H2 induction creates an environmental condition that favors rapid mastocytosis, which is critical in the elimination of parasites from the gastrointestinal tract. Our data on the site-selective loss of mast cells, as well as the different mechanisms that lead to immune phase–dependent mast cell production in PI3K$^{-/-}$ mice, show that mast cell development is controlled by complex spatio-temporal regulatory mechanisms. Future work to determine the regulatory mechanisms that control this system will contribute to our understanding of many physiological events that are mast cell–dependent.

Methods

Mice. Mice deficient in *Pik3r1* on a 129Sv × C57BL/6 background were as described[28,29]. *Pik3r1*$^{-/-}$ mice were then backcrossed to a BALB/c background for seven generations. PI3K$^{-/-}$ and PI3K$^{+/-}$ mice were obtained by intercrossing heterozygous (*Pik3r1*$^{+/-}$) female mice with homozygous (*Pik3r1*$^{-/-}$) male mice. The genotypes of litters were determined by PCR analysis of genomic DNA with primers specific for *Pik3r1* and the neomycin-resistance gene. Wild-type BALB/c and WBB6F1 *W/W*^{v} mice were from Sankyo Labo Service Co. (Tokyo, Japan) or Taconic (Germantown, NY). All mice were maintained under specific pathogen–free conditions in Taconic or our animal facilities. All experiments were done in accordance with our Institutional Guidelines.

Antibodies, cytokines and reagents. Monoclonal antibody to PI3K p85α was from Upstate Biotechnology (Lake Placid, NY). Antisera to PI3K p50α and p55α were as described[28]. Antisera to PI3K p110α, p110β, p110δ, Erk2 and p38α were from Santa Cruz Biotechnology (Santa Cruz, CA). Rabbit polyclonal anti–phospho-PKB, anti-PKB and mouse monoclonal anti–phospho Erk (p42/44) were from Cell Signaling Technology (Beverly, MA). Fluorescein isothiocyanate (FITC)-conjugated monoclonal anti–mouse IgE and phycoerythrin (PE)-conjugated monoclonal anti–c-Kit were from Pharmingen (San Diego, CA). Murine recombinant IL-3 (rIL-3) was a gift of A. Miyajima (University of Tokyo) or from PeproTech (London, UK). Murine rSCF, rIL-4 and rIL-10 were also from PeproTech. LY294002 was from Calbiochem (San Diego, CA). RPMI 1640 (Gibco-BRL, Gaithersburg, MD) supplemented with 10% fetal calf serum (FCS, HyClone, Logan, UT), 2-mercaptoethanol (50 μM), L-glutamine (2 mM), penicillin (100 U/ml), streptomycin (100 μg/ml) and sodium pyruvate (1 mM) was used as complete culture medium (CM).

Experimental septic peritonitis. For experimental septic peritonitis, mice were intraperitoneally injected with dose-determined enterobacteria in 1 ml of PBS (A_{600} 0.10–0.12). Enterobacteria were prepared from the ceca of female BALB/c mice by culturing in Luria Broth (LB) liquid medium (Gibco-BRL) at 37 °C overnight. The dose of bacteria was determined by a spectrophotometer (DU 640; Beckman, Palo Alto, CA) and adjusted to A_{600} 0.10–0.12 in PBS. To examine the number of bacteria that survived in the peritoneum, peritoneal washing fluid (PWF) was obtained by washing peritoneal cavities with 5 ml of PBS 3 h after infection. The PWF was then serially diluted, spread on LB plates and incubated at 37 °C. After overnight incubation, the number of bacterial colonies was counted as the number of bacteria surviving in the peritoneum. The data are presented as colony-forming units (CFU) per 1 ml PWF. PWF was also tested for the amount of TNF-α released in peritoneal cavities 1 h after infection. Titers of TNF-α were determined by a specific enzyme-linked immunosorbent assay (ELISA).

Histochemistry, enzyme cytochemistry and flow cytometry. To observe tissue mast cells, 6-μm paraffin sections of fixed tissues were stained with safranin and 1.0% alcian